NCMRWF

NMRF/RR/01/2011

RESEARCH REPORT

Tropical cyclone prediction using different convective parameterization schemes in a mesoscale model

Saji Mohandas and R. G. Ashrit

June 2011

National Centre for Medium Range Weather Forecasting
Ministry of Earth Sciences
A-50, Sector 62, NOIDA – 201307, INDIA

Tropical cyclone prediction using different convective parameterization schemes in a mesoscale model

Saji Mohandas and R. G. Ashrit

June 2011

National Centre for Medium Range Weather Forecasting
Ministry of Earth Sciences
A-50, Sector 62, NOIDA – 201307, INDIA

Earth System Science Organisation

National Centre For Medium Range Weather Forecasting

Document Control Data Sheet

S.No.		
1	Name of the Institute	National Centre for Medium Range Weather Forecasting (NCMRWF)
2	Document Number	NMRF/RR/01/2011
3	Date of publication	June 2011
4	Title of the document	Tropical cyclone prediction using different convective parameterization schemes in a mesoscale model
5	Type of Document	Research report
6	No.of pages & figures	57 pages, and 32 figures
7	Number of References	36
8	Author (S)	Saji Mohandas, R. G. Ashrit
9	Originating Unit	National Centre for Medium Range Weather Forecasting (NCMRWF), A-50, Sector-62, Noida, Uttar Pradesh
10	Abstract (100 words)	The current study presents the characteristics of cumulus parameterization schemes (CPS) used in real time prediction of three cases of tropical cyclones in the north Indian Ocean. The study makes use of the Weather Research and Forecasting model of Non-hydrostatic Mesoscale Model version (WRF NMM) with a horizontal resolution of 27Km. The four deep cumulus schemes studied are (a) Modified Kain-Fritsch (KF) (b) Betts-Miller-Janjic (BMJ) (c) Simplified Arakawa-Schubert (SAS) and (d) Grell Devnvyi Ensemble (GD) schemes.
11	Security classification	Unrestricted
12	Distribution	General

Contents

Abstract

The current study presents the characteristics of cumulus parameterization schemes (CPS) used in real time prediction of three cases of tropical cyclones in the north Indian Ocean. The study makes use of the Weather Research and Forecasting model of Non-hydrostatic Mesoscale Model version (WRF NMM) with a horizontal resolution of 27Km. The four deep cumulus schemes studied are (a) Modified Kain-Fritsch (KF) (b) Betts-Miller-Janjic (BMJ) (c) Simplified Arakawa-Schubert (SAS) and (d) Grell Devnvyi Ensemble (GD) schemes. Three cases chosen for the study are unique cases with entirely different characteristics, synoptic conditions and with varying levels of performance of the driving global model forecasts. The objective of the current study is to report the relative performance of the CPS schemes and to demonstrate the impact of the synoptic conditions as reflected in the initial and boundary conditions. The study compares the cyclone tracks, intensification, the associated rainfall patterns, standard verification scores and the contribution of grid-scale precipitation towards the total rainfall by the mesoscale model between the different cases as well as the different cumulus parameterization schemes. The performance of the tropical cyclone real-time predictions by the mesoscale model depends not only on the model physics but also on the synoptic conditions.

1. Introduction

The current study addresses the questions like, how well certain parameterisation schemes perform under a variety of synoptic conditions and in the high resolution mesoscale models. There are systematic studies comparing the performance of deep convective parameterisation schemes in high resolution Fifth-generation NCAR/Penstate Mesoscale Model (MM5) (Wang and Seaman, 1997; Ma and Tan, 2009; Yang and Tung, 2003, Stensrud et al., 2000). There are a couple of recent studies using MM5 or Weather Research and Forecasting (WRF) models on the impact of parameterization schemes on heavy rainfall events and weather systems over Indian ocean (Rao and Prasad, 2007, Vaidya, 2007, Vaidya and Kulkarni, 2007, Deb et al., 2008). There are a wide variety of cumulus parameterization schemes that are developed and tested for limited number of convective environments and horizontal resolutions (Kuo et al. 1996; Gallus, 1999; Peng and Tsuboki, 1997; Yang et al., 2000, Spencer and Stensrud, 1998). A focused study on the sensitivity of these schemes on the behaviour of the Indian Ocean Tropical Cyclone forecasts for a particular scale and a particular resolution is attempted here. Three cases of tropical cyclones which sustained their intensity for at least four or five days have been selected for the current study. They are Gonu (1 – 7 June 2007), Sidr (10 – 16, November, 2007) and Nargis (26 April – 3 May, 2008). Section 2 describes the methodology and the data used.

The focus of the study is on the associated characteristics of the TC forecasts in relation to the Cumulus Parameterisation schemes (CPS), which is the only difference between the set of experiments. Though the explicit simulation of individual cloud cells requires a resolution of the order of at least a few hundred meters, some gross dynamic features associated with the mesoscale convective systems (MCS) can be identified using models with a resolution of a few tens of kilometers. A reasonable partition between the subgrid-scale and resolvable rainfall is crucial to produce realistic representation of precipitation events. Over two-thirds of MCS rainfall is convective as opposed to stratiform (Houze, 1977; Johnson and Hamilton, 1988) and the deep convective representation must be able to realistically estimate not only the convective rainfall but also the feedbacks on the surrounding environment that influence further convective development (Molinari and Dudek, 1992). Established studies of observed mesoscale phenomena indicate that

parameterized, moist downdrafts are crucial for reproducing many of the observed mesoscale characteristics as well as correct large scale temperature fields (Cram et al., 1992; Zheng et al., 1994; Stensrud and Fritsch, 1994). Also in some precipitation events, the characteristics of the precipitation can transform from predominantly convective to a resolvable mesoscale system as the systems mature (Dudhia, 1989; Zhang et al., 1989; Zhang and Gao, 1989). Thus the relative contributions of convective and nonconvective parts of the model rainfall output are also examined. The objective of the current study is to present the relative performance of the CPS schemes under different operational environments, which includes also the error in the initial location and the intensity of TCs in the initial analyses. A brief description of the synoptic conditions is given in section 3. The last two sections deal with the results and concluding remarks respectively.

2. Data and methodology

Weather Research and Forecasting model of Non-hydrostatic Mesoscale Model flavour (WRF NMM SI version 2.2) was used for real time prediction of the tropical cyclones. Analyses and forecasts of T254L64 global spectral model (Rajagopal et al., 1997) are used for the initial and boundary conditions as well as for verification. Tropical Rainfall Measuring Mission (TRMM) derived daily rainfall estimates are used for rainfall verification, which is the best reliable source over the oceanic areas (Simpson et al., 1996). Marchok et al. (2007) suggested a scheme for validating the quantitative precipitation forecasts in terms of the ability to match the observed rainfall patterns, the ability to match the mean value and the volume of the observed rainfall and the ability to produce the extreme amounts often observed in tropical cyclones. The verification statistics in the current study were generated following a similar principle of track-relative analysis, over a domain of 10x10 degree box centred around the estimated forecast locations of TCs. Thus the intent is to study the associated rainfall characteristics only rather than verification over the entire domain of integration. This strategy of verification does not ensure that the associated rainfall region is exactly superposed over the observed satellite-derived precipitation region during comparisons between the two. There can be instances when the entire pattern of observed rainfall can be partly or fully out of the domain of verification for a particular case or CPS scheme, reducing the skill score drastically. Average of all the skill scores will be mostly

very much different than the individual cases or with different initial conditions (ICs).

The deep convective schemes used are the modified Kain-Fritsch (KF: Kain, 2004; Kain and Fritsch, 1990, 1993), Betts-Miller-Janjic (BMJ: Betts and Miller, 1993; Janjic, 1994; 2000), Simplified-Arakawa Schubert (SAS: Pan and Wu, 1995; Grell, 1993; Grell et al., 1994) and Grell-Devenyi Ensemble scheme (GD: Grell and Devenvyi, 2002). All the experiments used common initial and boundary conditions. Fig. 1 shows the domain of integration with the orography. Table 1 describes the list of other physics options employed. No tuning of parameters was done to enhance its performance in any particular case. WRF NMM is run for 3 days at a resolution of 27 Km in the horizontal and 38 vertical levels with initial and boundary conditions interpolated from NCMRWF T254L64 model analyses and forecasts. All experimental runs are carried out without any mesoscale data assimilation or nudging. The number of initial conditions used for the experiments are 5 (1- 5 June, 2007) for Gonu, 4 (11-14 November, 2007) for Sidr and 6 (27 April – 2 May, 2008) for Nargis case as these are the dates for which corresponding track positions are available from India Meteorological Department (IMD) and the statistics are prepared with locations of systems at every 24 hour intervals with respect to IMD positions.

For all the three cases, the total sample size of integrations are 15 and for each field at each grid point, the values were taken at 24-hourly interval making a total of 15 analyses and 45 forecast values. The simulated prognostic fields of wind, minimum Sea Level Pressure (SLP) and rainfall were verified against the analyses and observed estimates. The 24-hour accumulated rainfall forecasts were evaluated against the TRMM rainfall estimates quantitatively using statistical skill scores (Bias Score BS, Threat Score TS and Equitable Threat Score ETS) with the threshold values of 10mm, 20mm… up to 90mm. Also the percentage contribution of non-convective precipitation over the total precipitation was also computed for each day of forecasts along with the averages. As the study looks into the aspects related to the different synoptic conditions, the composite average of all the statistics was presented for total, case wise and CPS-specific etc.

Table 1. Brief description of WRF NMM model.

Horizontal resolution: 0.24 deg (Appr:27Km), Vertical: 38 levels, Grid size: 160x250

Time-step: 60secs

Land surface Model : NOAH LSM with 4 soil levels

Surface Layer : Monin-Obukhov (Janjic)

Planetary Boundary Layer scheme : Mellor-Yamada-Janjic TKE

Longwave Radiation : GFDL (Eta) –invoked 3 hourly

Shortwave Radiation : GFDL (Eta) –invoked 3 hourly

Microphysics: Ferrier (New Eta)

Deep Convection: Kain-Fritch (New Eta)

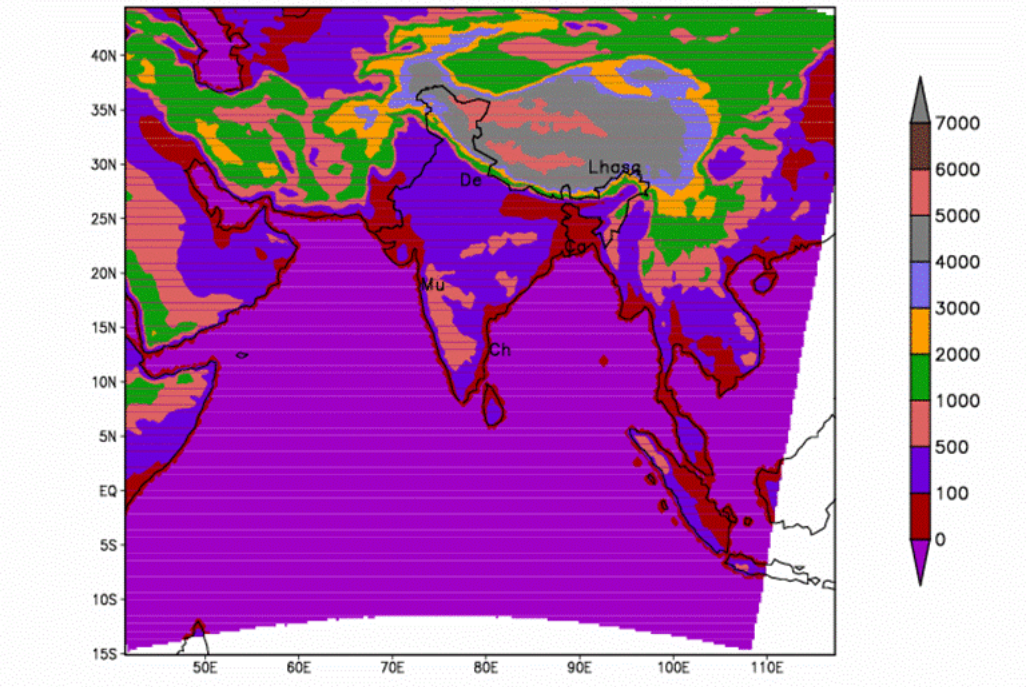

Fig. 1 Domain of integration of WRF NMM model, along with orography in meters (shading).

3. Case description

The three systems selected for the study show distinct characteristics in genesis and movement. The tropical cyclone Gonu developed as a depression over the east central Arabian Sea on 1 June, 2007. It moved mainly westwards and northwestwards, ultimately intensifying into a super cyclonic storm and crossed the Makran coast on 7 June, 2007 as a cyclonic storm. The minimum SLP reported is 920.0 hPa at 15z on 4th June, 2007 with an estimated maximum wind speed of 127 Kts. The Tropical cyclone Sidr developed over southeast Bay of Bengal as a depression on 12 November, 2007, mainly moving northwestwards and northwards, and crossed Bangladesh in the evening of 15 November, 2007. The minimum SLP was 944.0 hPa on 15th November with a maximum wind speed in the spiral bands estimated to be 115Kts. The tropical cyclone Nargis also developed over south central Bay of Bengal by 27 April, 2008 and initially moved northwestwards till 28th, thereafter northwards. By 30th, it recurved and moved northeastwards, intensifying and reaching Myanmar coast by 2 May, 2008. It crossed the coast on 2 May, 2008 and thereafter moved east northeastwards, weakening by 3 May, 2008. On 2nd May, 2008, it attained a minimum SLP value of 962.0 hPa and a maximum wind speed estimates of 90 Kts.

The three TCs formed in three different seasons. Gonu developed during the monsoon onset period, delaying the onset of Monsoon 2007 and is a rare case of supercyclone developed over Arabian Sea. Sidr formed over South Bay of Bengal during the post monsoon period and Nargis formed over southeast Bay of Bengal during the pre-monsoon period. All of them have origins in different ocean basins and followed totally distinct tracks and landfall patterns; Gonu moved northwestward striking the gulf countries, Sidr more or less northwards striking Bangladesh and Nargis first west northwestwards and then recurving towards Myanmar coast. Each of them displays different patterns and timeline of development, intensification and decay as well as each of them were driven by different steering currents. Thus each of them is unique in all the aspects and all of them occurred within a period of one year (June 2007 – May 2008). These differences in the environmental conditions, cyclone basins of genesis and the accuracy of initial and boundary conditions are also reflected in the performance and track errors of the mesoscale models. Nonetheless, the focus of these forecast experiments is on the sensitivity of these factors on the behaviour of

the various cumulus parameterizations schemes used at the particular resolution of the model under study.

It is important to discuss the performance of the driving T254L64 model analyses and forecasts before assessing the mesoscale models. A brief summary of the track error and the errors in the intensity (minimum SLP and maximum wind speed) during the peak intensity period of the tropical cyclone in the T254L64 analysis and forecast is presented in Table 2. It can be seen that Sidr is having maximum track error (394Km) in day-3 forecast though the initial condition has the least error (59Km). The wind speed is grossly underpredicted by T254L64 analysis and forecasts in both cases. The large difference in the errors in the minimum SLP between Nargis and Sidr cases is partly due to the difference in the observed intensity between the systems in terms of the dip in the minimum SLP which was not reflected by the global model analyses and forecasts. In other words the Sidr cyclone (with a minimum SLP of 956hPa) was more intense than Nargis (with a minimum SLP of 972hPa) as per the IMD records, whereas T254L64 analysis and prediction produced tropical cyclones with comparable intensity (as obvious from the errors given in the Table 2). Initial locations and strength of the cyclone Gonu have maximum errors from the observations. However, the intensity of Gonu is very much underpredicted by the global model, so much so that it can not be termed as a TC rather seen as a depression. At the same time the global model performance of Nargis is the best among the three with its least error in the case of minimum SLP, its correct prediction of a recurving track and the subsequent movement towards Myanmar fairly well in advance. Hence it can be generally concluded that T254L64 performance was generally better in the case of Nargis than Sidr. When compared with Gonu, though the day-3 track error of Gonu is comparable with the other two cases, the initial centre location error is much large and the model could not reproduce the intensity of the circulation anyway near the observed either in the analysis or in the forecast.

Table 2. Errors of T254L64 analysis and day-3 forecast in track (km), maximum wind speed (knots) and minimum central pressure (hPa) valid on the day of maximum intensity. (Errors are computed from the IMD observations.)

TC system (valid day)	Track (Km)		Maximum Wind speed (kts)		Minimum Pressure (hPa)	
	Analysis	Day-3 fcst	Analysis	Day-3 fcst	Analysis	Day-3 fcst
Nargis (02 May 2008)	115	341	-44.4	-42.7	25.2	25.8
Sidr (15 November 2007)	59	394	-46	-40.3	46.2	41.5
Gonu (05 June 2007)	147.6	300.2	-84	-88.7	64	63.1

4. Results and discussions

4.1 Track and movement

The model runs are carried out using multiple initial conditions for each case of cyclones as described in Section 3. Figs. 2 & 3 show the tracks of the systems, Gonu and Sidr, for all the four deep convection schemes along with the corresponding T254L64 analysis positions. For Fig. 4, comparison of six runs made for Nargis cyclone have been done against the observed IMD positions. Though many of the characteristics can be generalized in comparison between the deep convective schemes cutting across the tropical cyclone cases, the individual tracks of the cases vary day by day and the forecast positions are also more dependent on the performance of its driving model T254L64. The first impression one can make from the panels is that the cyclone in the model experiments is moving rather too slow compared to the observations. Besides, the predicted positions are clustered around the observations in the early stages of the run and the dispersion increases as the forecast progresses.

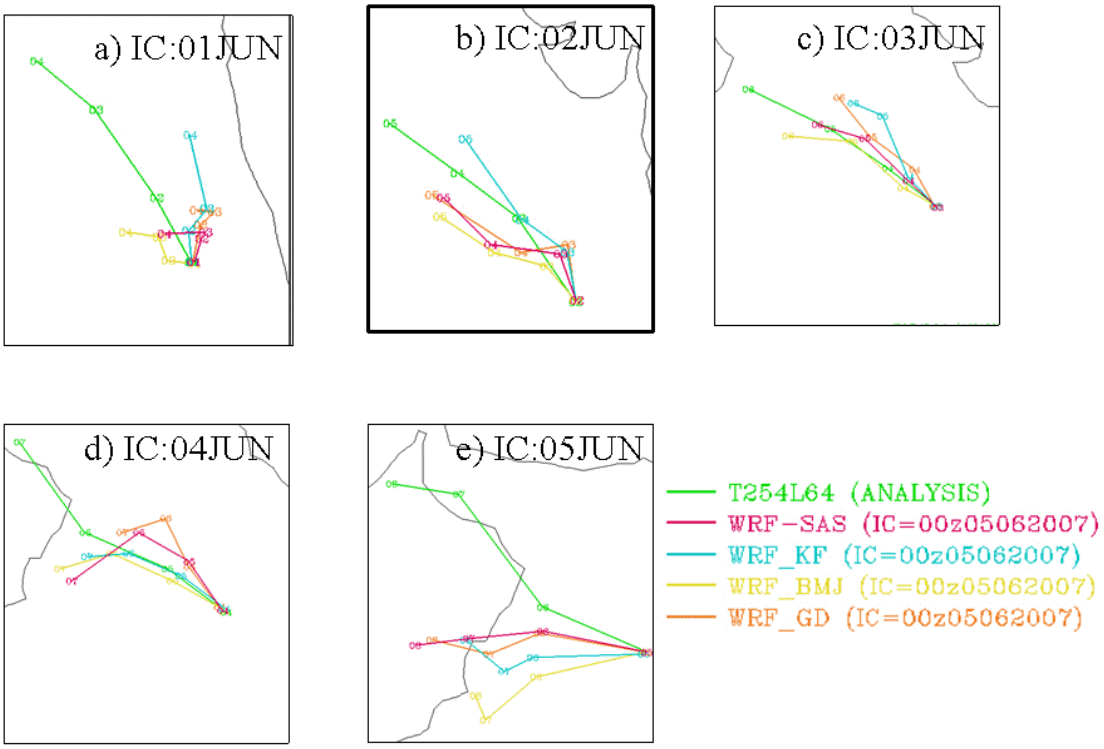

Fig. 2 Tracks (colored curves) of the Gonu cyclone forecasts (a-e) by WRF NMM with initial conditions (ICs) of 00Z 01- 05 June, 2007, with four cumulus parameterization schemes (CPS) KF, SAS, BMJ and GD, starting with the analysis and upto day-3 forecasts, along with T254L64 analysis positions.

Fig 5a shows the composites of predicted track errors for each of the cumulus parameterization schemes and Fig 5b for each cyclone case. The composites are computed for each day by averaging track errors from all model runs. It can be seen that KF produces the least errors averaged across all cases, though not much difference is seen on averaging for all the forecast lead times between KF, SAS and GD. Also, BMJ performed poorest among the four when averaged across all the three cases. It can also be seen that Sidr shows the maximum track error followed by Gonu in day-2 and day-3, whereas for day-1 forecasts there is not much difference in the forecast errors in all the three cases in spite of the fact that Sidr is having the least initial error at t=0.

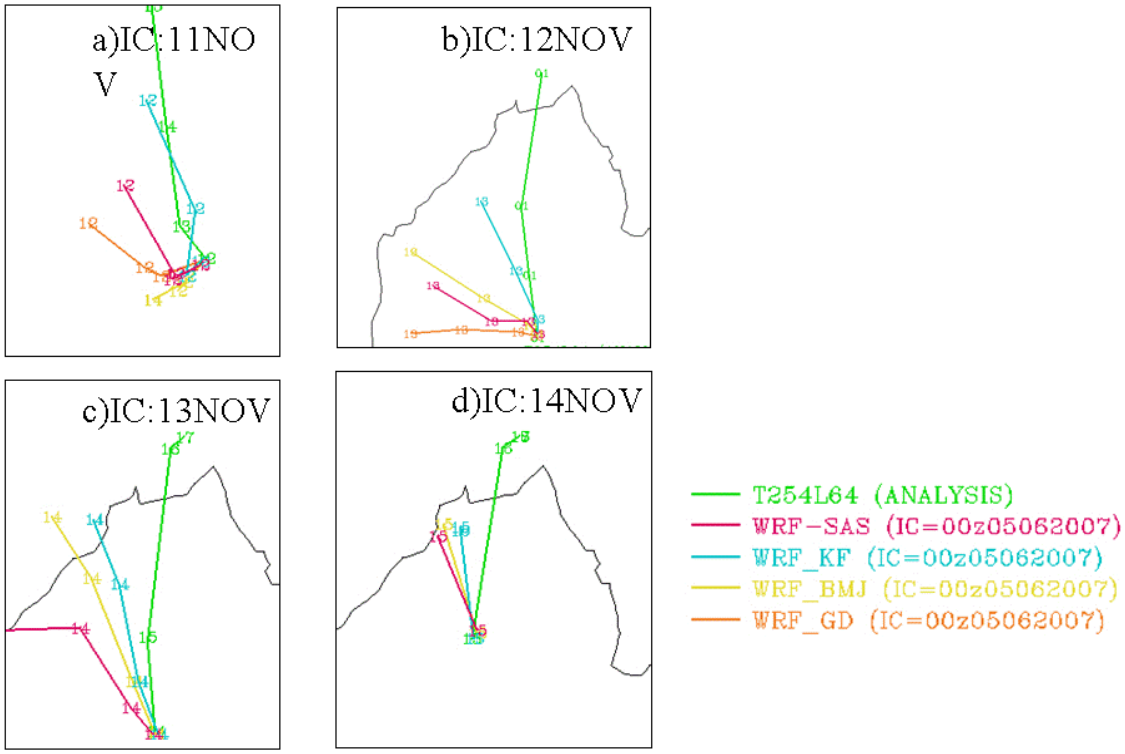

Fig. 3 Similar to Fig. 2, but (a-d) for Sidr cyclone with ICs 00Z 11-14 November, 2007.

The poor track predictions for Gonu and Sidr are apparently because of the initial location or intensity errors as well as the errors in the tracks predicted by the driving global model. Nargis track predictions are the best among all the three cases, though Sidr has the least mean IC errors. Though initial conditions are a little off from the observed positions on 27th and 28th for the Nargis cyclone, the direction of movement and the day-3 positions are quite well predicted by KF in general compared to the other three CPS schemes, which is also true for all the three cases. The performance between the four CPS schemes does not differ much for Nargis case when the errors in the initial positions and intensity are the least. It is worth mentioning a fact here that GD failed to predict a strong cyclonic system in many of the instances and the centre itself was not clear enough to locate it, which rules out any fair comparison with the other CPS schemes.

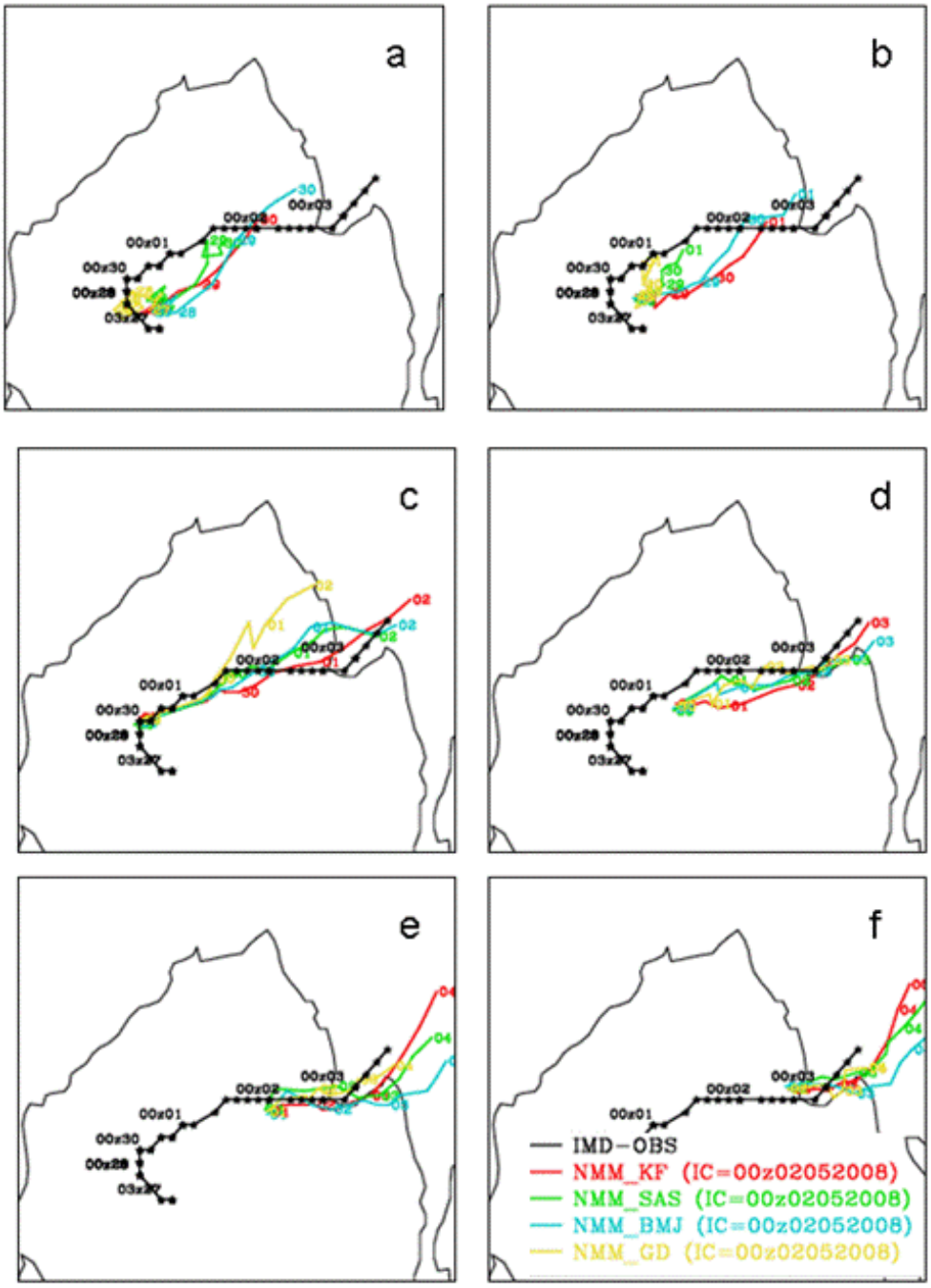

Fig. 4 Similar to Fig. 2, but (a-f) for Nargis cyclone, with ICs 00Z 27 April - 02 May, 2008, and along with the IMD observed track (dark curve) in place of T254L64 analysis track.

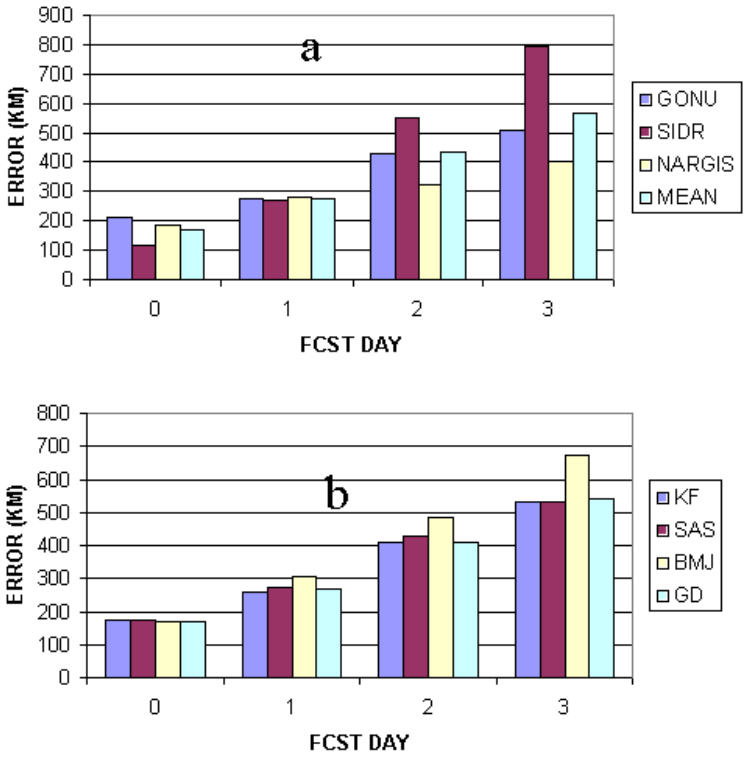

Fig. 5 Composite track errors in kilometers for analysis, day-1, day-2, and day-3 forecasts (a) for Gonu, Sidr and Nargis along with mean error averaged across runs with four CPS schemes and (b) separately for four CPS schemes (KF, SAS, BMJ and GD) averaged across all the three systems. Errors are computed from the observed IMD locations.

4.2 Intensity and associated rainfall

Here we briefly discuss the circulation vis-à-vis rainfall in the experiments for each of the three cases. Figures 6, 8 and 10 (7, 9 and 11) show forecast 850hPa geopotential and wind (daily rainfall) for the cyclones Gonu, Sidr and Nargis, respectively at mature stage. The four panels (a-d) in each of the figures correspond to the four experiments, namely, KF, SAS, BMJ and GD respectively. The panel e corresponds to T254L64 analysis (TRMM estimates) in the case of geopotential and wind (daily rainfall). Day-3 forecasts are shown for Gonu (because of the poor initial and boundary conditions for Gonu it took 3 days to peak in intensity) whereas day-2 forecasts are shown for Sidr and Nargis. The figures 6, 8, and 10 show clearly that, KF generally produces the strongest system in terms of intensity

and maximum wind speed, whereas GD is the weakest. Similarly the corresponding rainfall prediction (Figs. 7, 9 and 11) displays the maximum amount of accumulated rainfall predicted by KF, followed by SAS and BMJ, whereas GD shows the least amount of rainfall with hardly any contour greater than 8cms in the case of Nargis, the most intense among the three. Also it can be seen that KF produces the maximum mesoscale variations in the accumulated precipitation values, whereas, BMJ and SAS give hardly any mesoscale variability. GD on the other hand produces too much of the mesoscale variability with very broad and patchy rainfall bands of very smaller amounts. For Nargis case, though on an overall, the rainfall pattern of BMJ is similar to the TRMM satellite estimates (panel e) even without the associated spatial variability, the location of the maximum rainfall contour is partly over land whereas in TRMM the land rainfall is comparatively very less as the major rainfall patch is just off the coast.

Fig. 12 shows the minimum sea level pressure predicted by the four convective schemes, which is a statement of the predicted intensity starting with the same analysis, for Gonu (leftmost column a-d), Sidr (middle column e-h) and Nargis (rightmost column i-l). This shows that in general Gonu was the most under predicted and Nargis was the best predicted in terms of the intensity. It can be seen that, KF is the best in showing a tendency for intensification in the forecasts for Gonu and Sidr cases, whereas for Nargis case, its prediction is more or less matching with the IMD estimates. Among the other three schemes, SAS is the second best, though lagging far behind KF, whereas, BMJ and GD fare very poorly in matching the observed intensity. Exactly similar conclusion can be drawn for the maximum wind speed predicted by the system around the centre of the system (Fig. 13). Most of the conclusions as above can also be derived from the charts of wind speed and 24-hr. accumulated precipitation averaged over the 10x10 deg. grid box surrounding the forecast centres of the cyclones (Figs. 14 & 15).

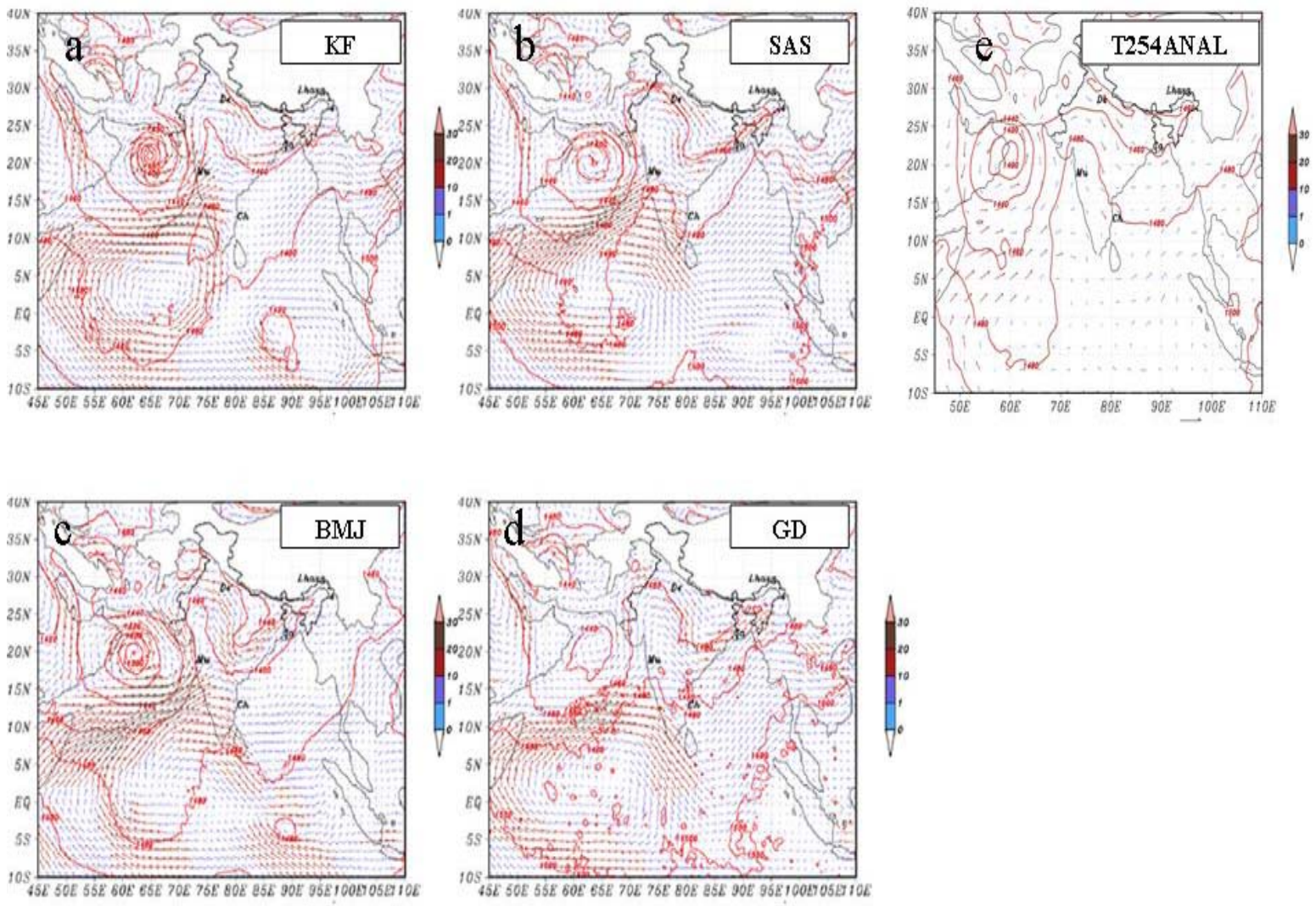

Fig. 6 Geopotential (m) contours and wind (m/s) arrows for the day-3 forecast valid for 06 June, 2007 using WRF NMM model with CPS schemes (a) KF (b) SAS (c) BMJ and (d) GD, along with (e) T254L64 verifying analysis.

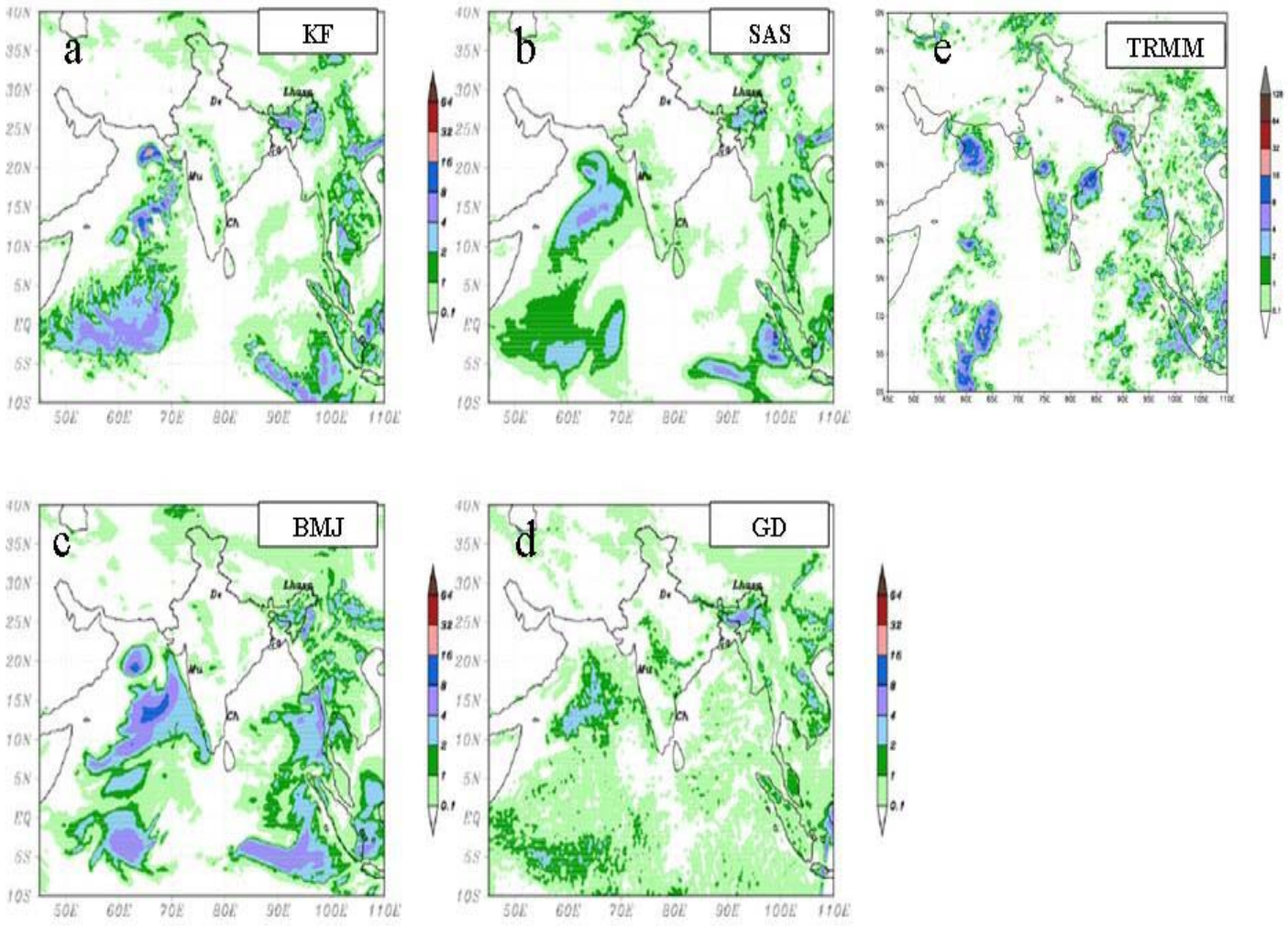

Fig. 7 Similar to Fig.6 for panels (a-d), but for previous 24-hour accumulated rainfall (cm- shading) valid at 00Z 06 June, 2007 and along with (e) TRMM 3B42RT derived daily rainfall estimates.

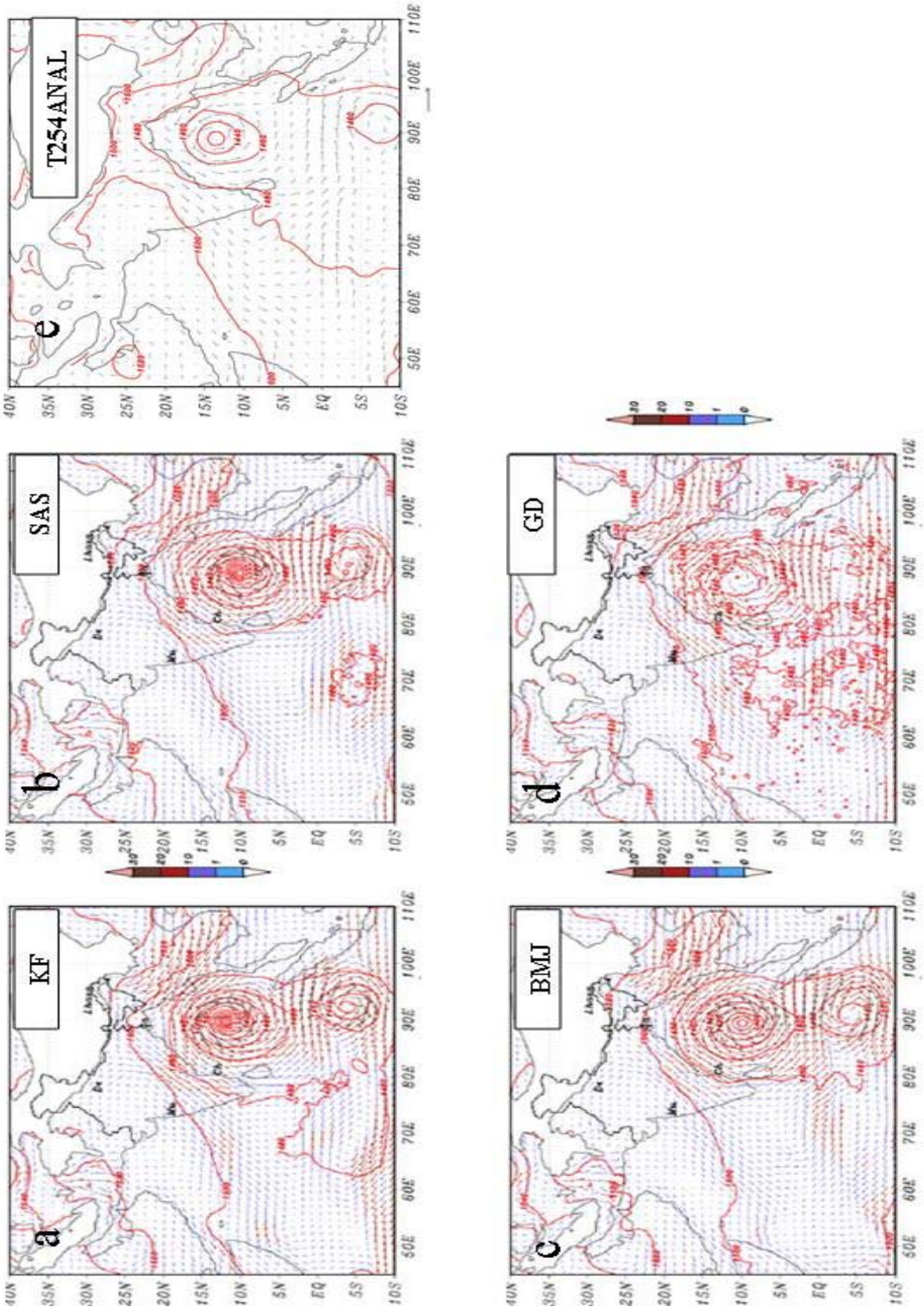

Fig. 8 Similar to Fig. 6, but for day-2 forecasts of Sidr valid at 00Z 14 November, 2007.

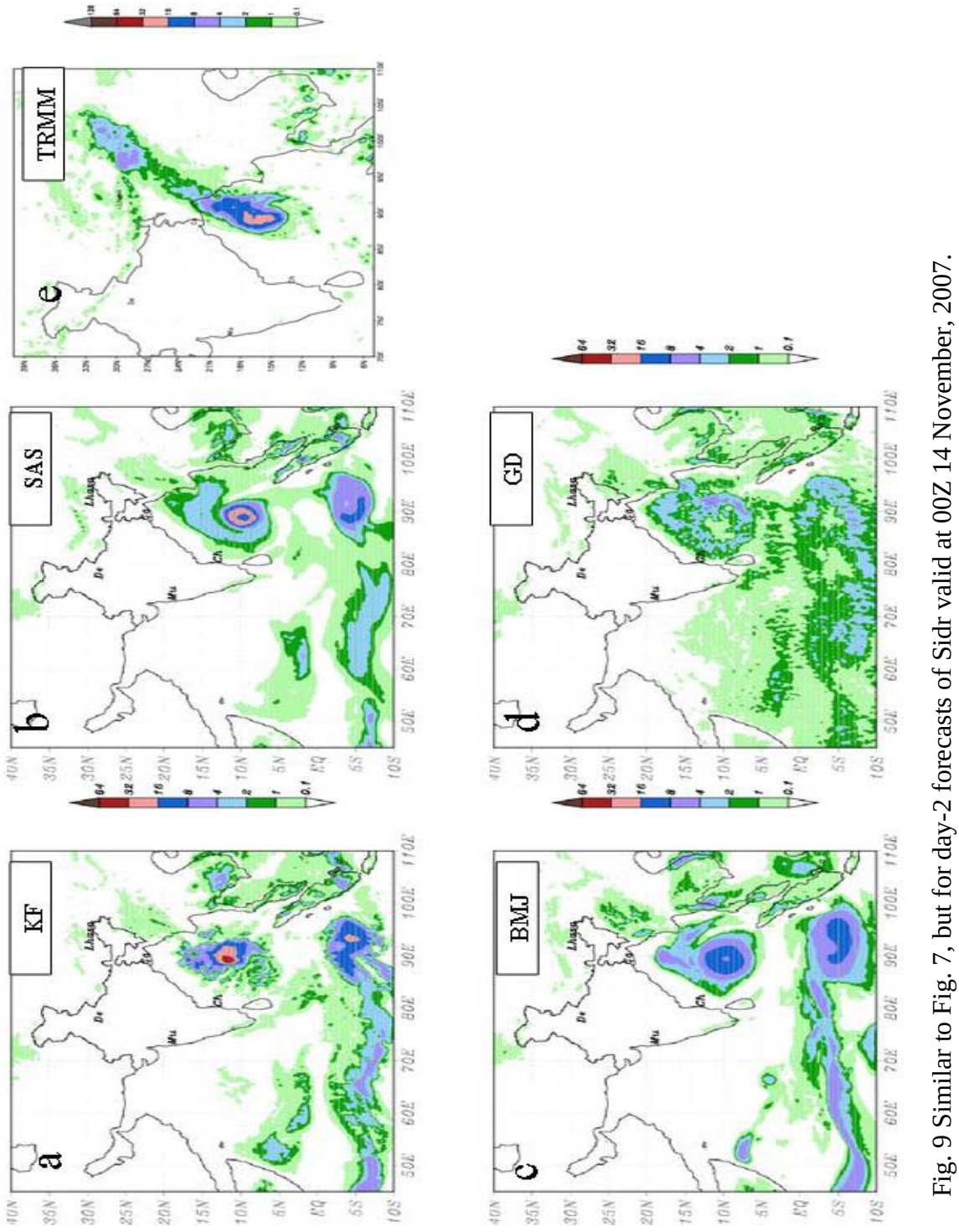

Fig. 9 Similar to Fig. 7, but for day-2 forecasts of Sidr valid at 00Z 14 November, 2007.

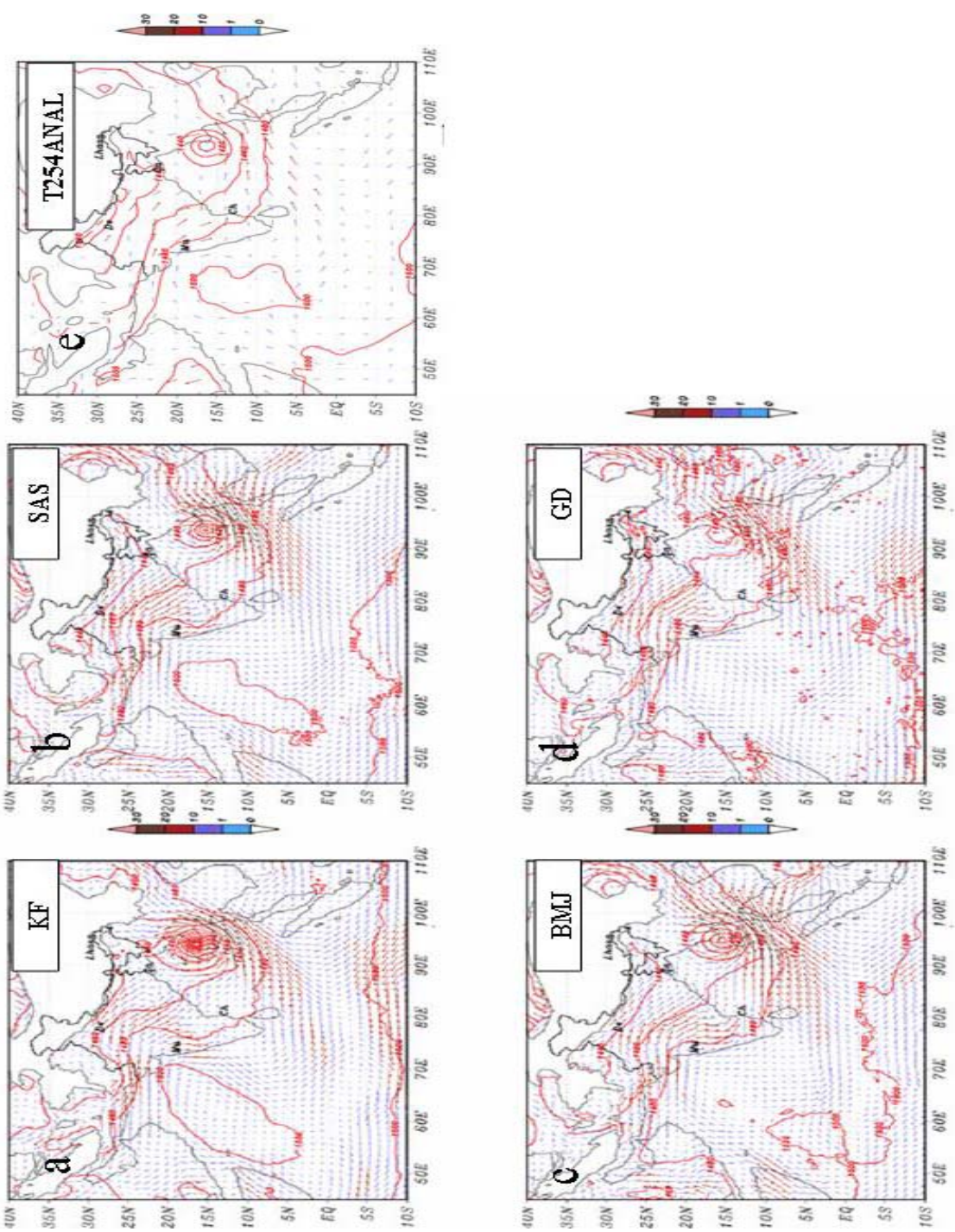

Fig. 10 Similar to Fig. 6, but for day-2 forecasts of Nargis valid at 00Z 02 May, 2008.

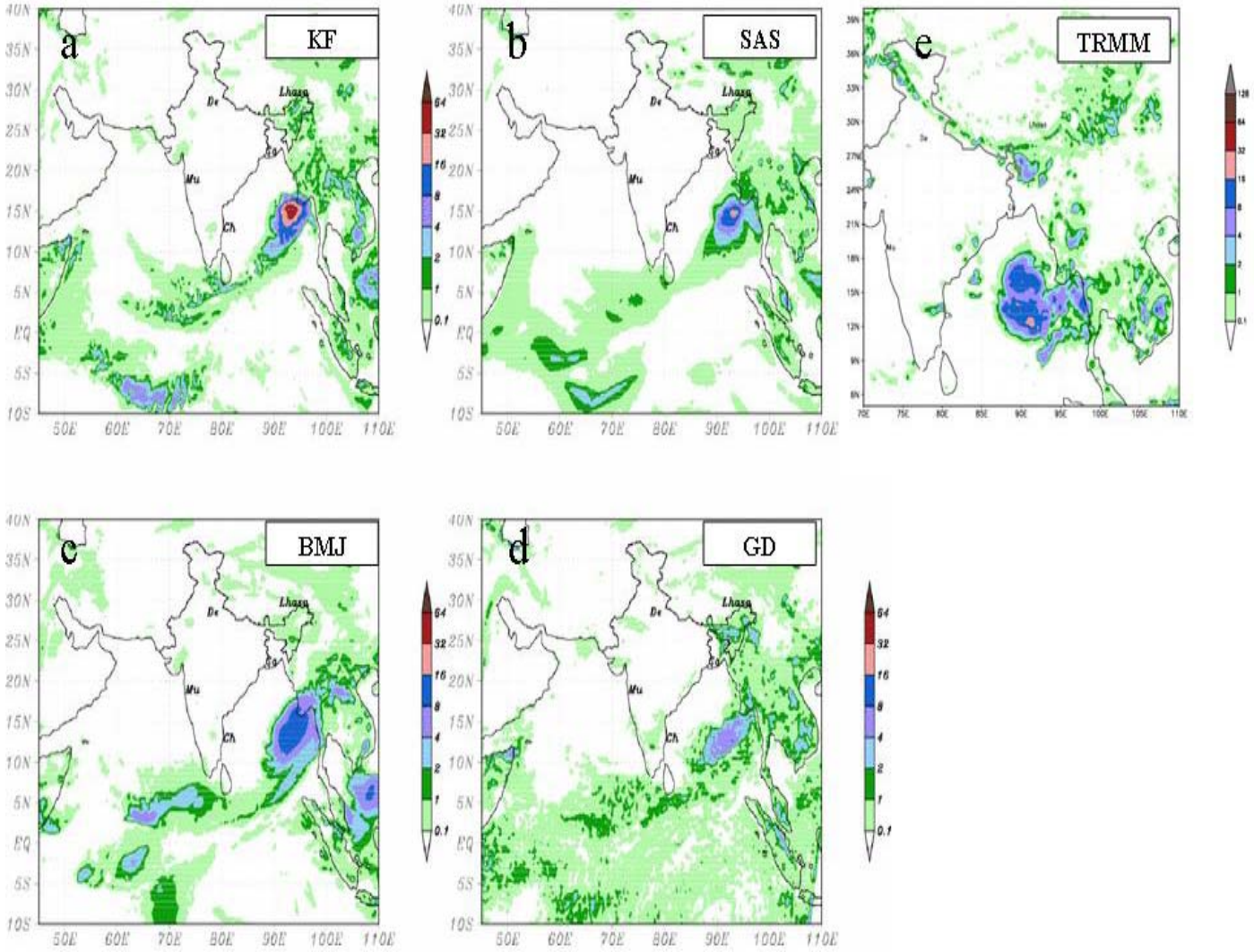

Fig. 11 Similar to Fig. 7, but for day-2 forecasts of Nargis valid at 00Z 02 May, 2008.

The intensity and the spread of the rainfall produced by the systems on predicted tracks can be estimated by the maximum grid point rainfall accumulated for the previous 24 hour period in the corresponding grid boxes in Fig. 16. Figures 17-19 show the averaged daily rainfall comparisons with the curves for day-1, day-2 and day-3 forecasts along with the TRMM estimates. KF scheme is seen to produce over prediction of associated rainfall with better input data and initial conditions, like Sidr and Nargis. While for Gonu it is able to intensify the system so that the rainfall is more or less matching with the observed TRMM estimates. For GD it is gross under prediction of intensity and rainfall for all the cases except Sidr. For Sidr, the rainfall in the 10x10 degree box is more or less matching with the observed TRMM derived daily estimates. For Nargis case the averaged rainfall for SAS is a better match with the TRMM estimates

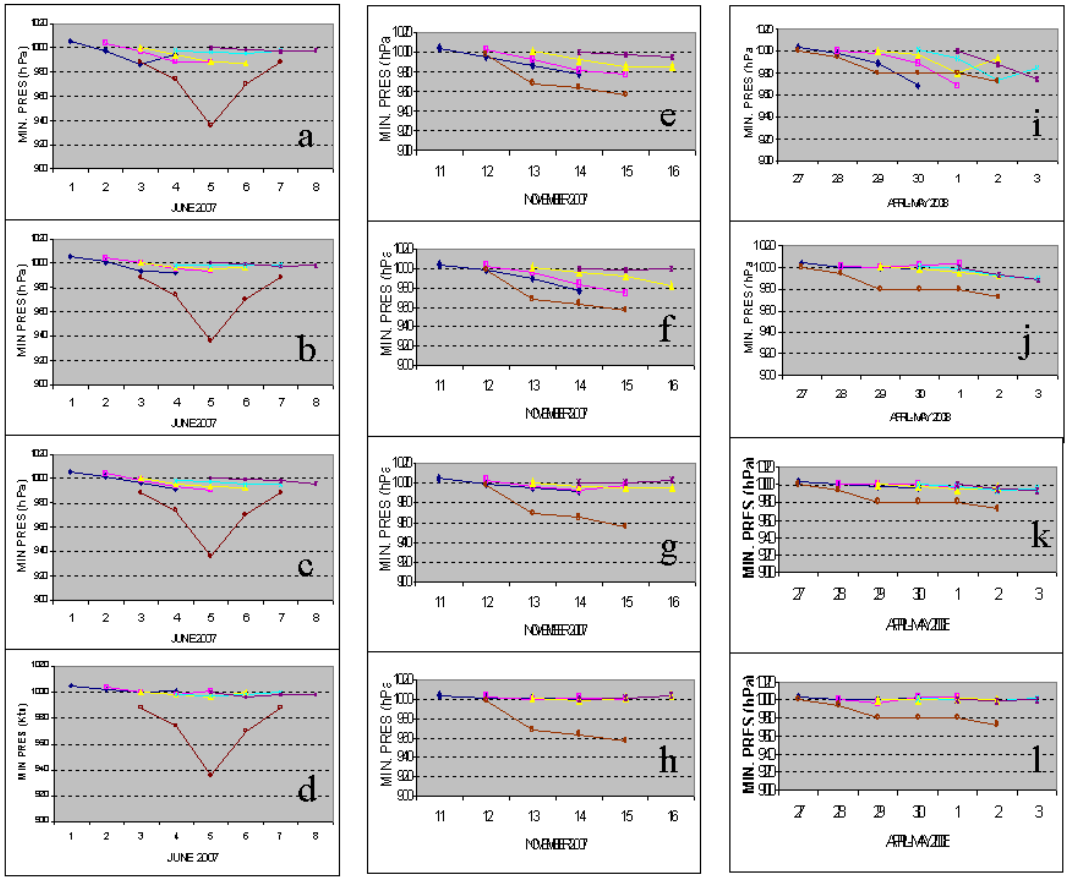

Fig. 12 Minimum central sea level pressures (hPa) in the 10x10 degree box around the predicted centres of TCs by WRF NMM model 3-day runs with different ICs with four CPS schemes for Gonu (a-d), Sidr (e-h) and Nargis (i-l), along with the IMD observation.

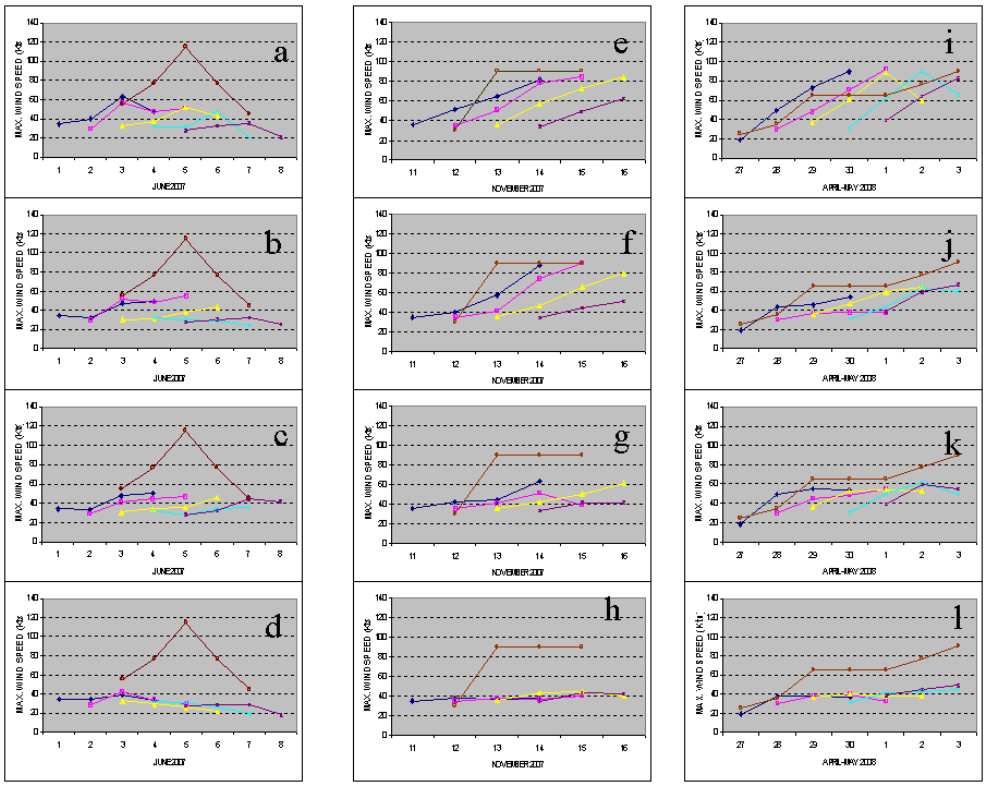

Fig. 13 Similar to Fig. 12, but for maximum wind speed (knots) in the box area.

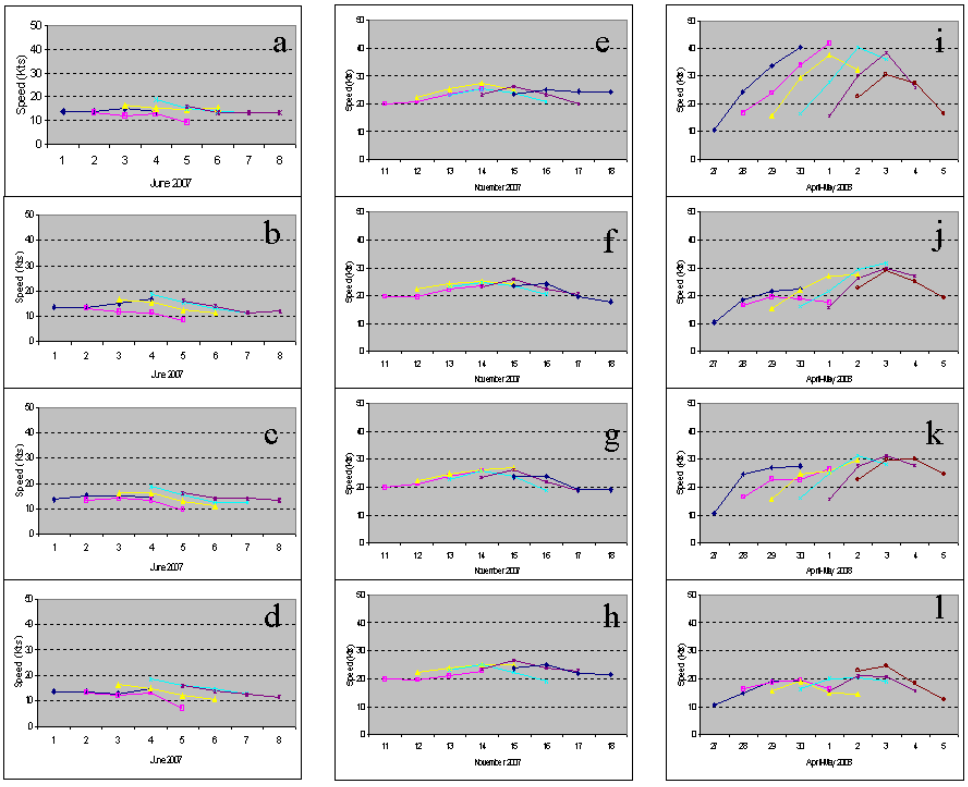

Fig. 14 Similar to Fig. 12, but for average wind speed (knots) in the box area.

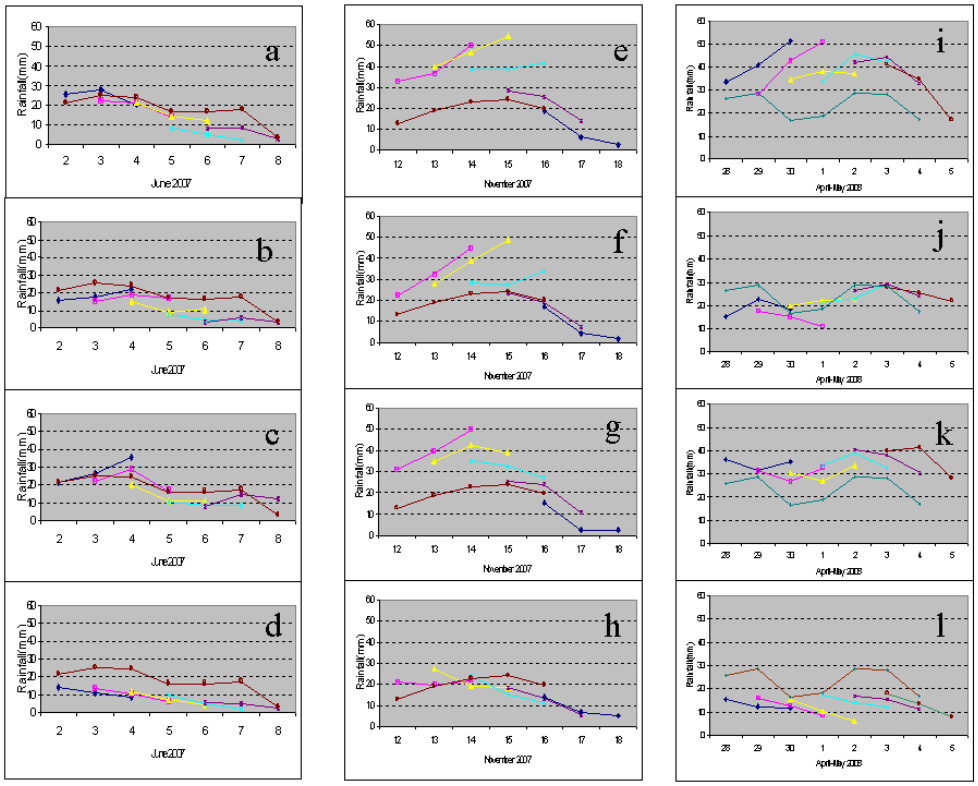

Fig. 15 Similar to Fig. 12, but for average 24-hourly rainfall (mm).

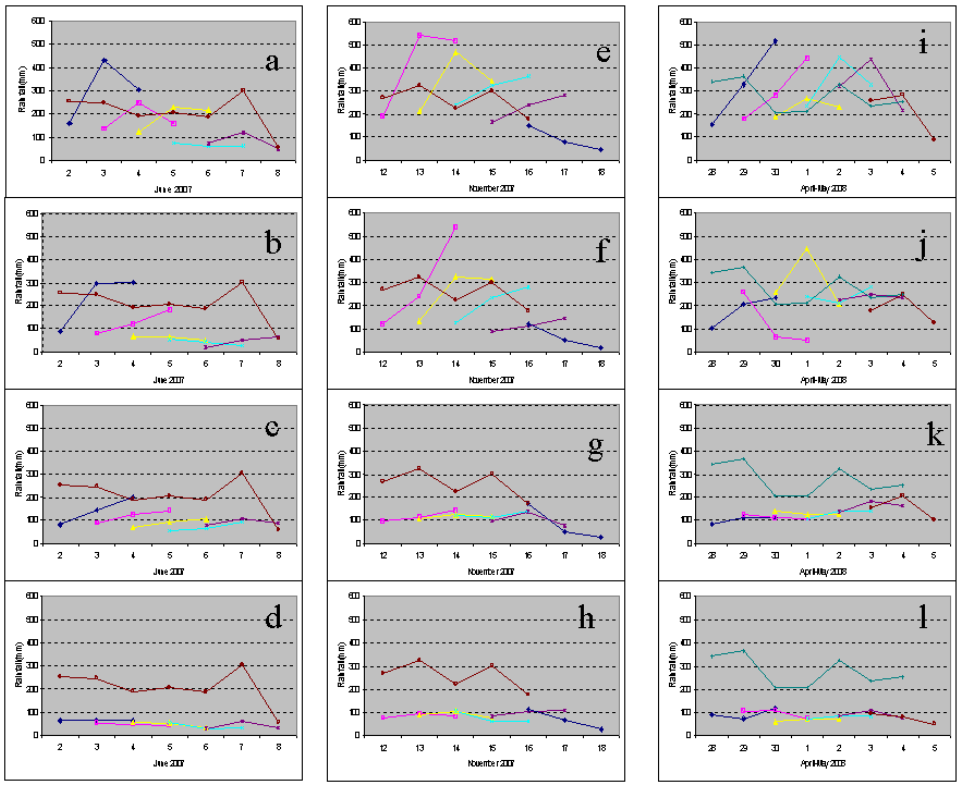

Fig. 16 Similar to Fig. 12, but for maximum 24-hourly rainfall (mm) in the box area.

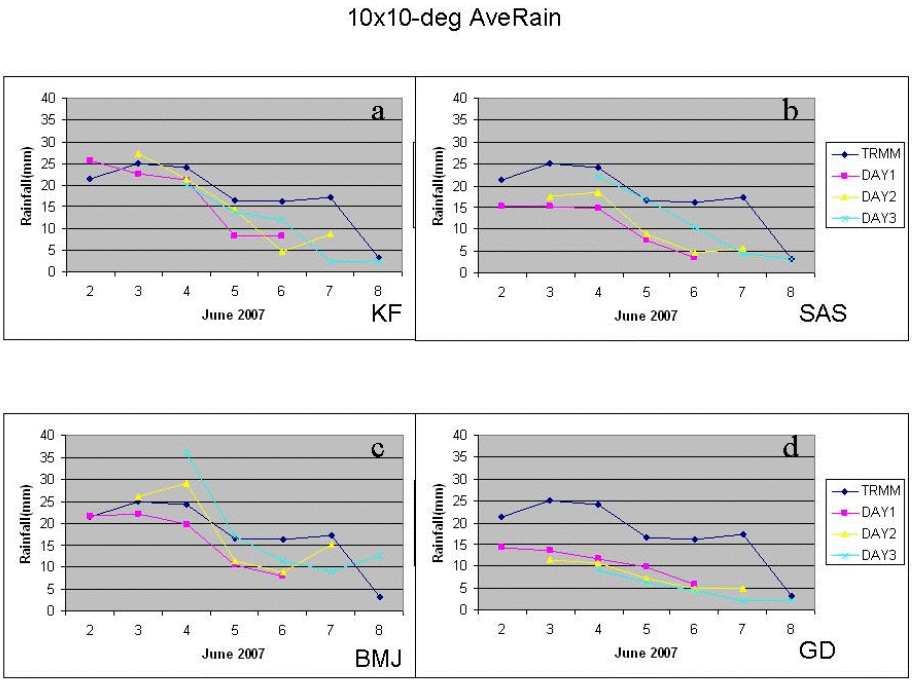

Fig. 17 Curves of box-averaged rainfall (mm) for day-1, day-2 and day-3 forecasts by WRF NMM model runs with four CPS schemes (a-d), along with the TRMM 3B42RT derived daily estimates in the same box corresponding to the forecast centres for Gonu.

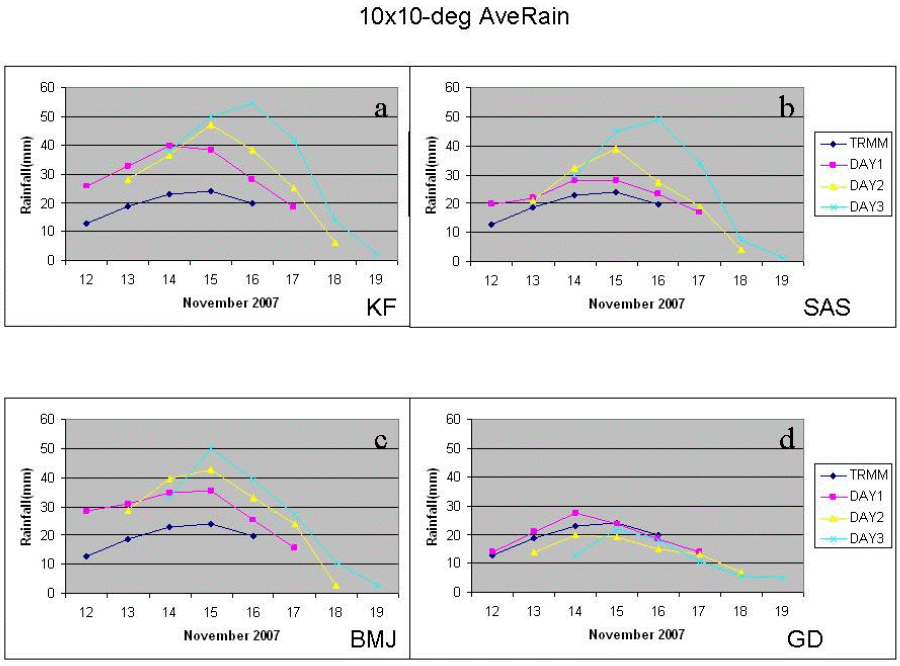

Fig. 18 Similar to Fig. 17, but for Sidr.

whereas for KF, there is an over intensification and over prediction. However, it has to be kept in mind while analyzing these results that the rainfall associated with the predicted TC is compared with the TRMM rainfall over the same domain, where as the peak rainfall and the geographical patterns of the observation may be a little bit shifted from those of the forecasts. Thus only the rainfall captured in the predicted box is used for averaging and the pattern matching is not carried out.

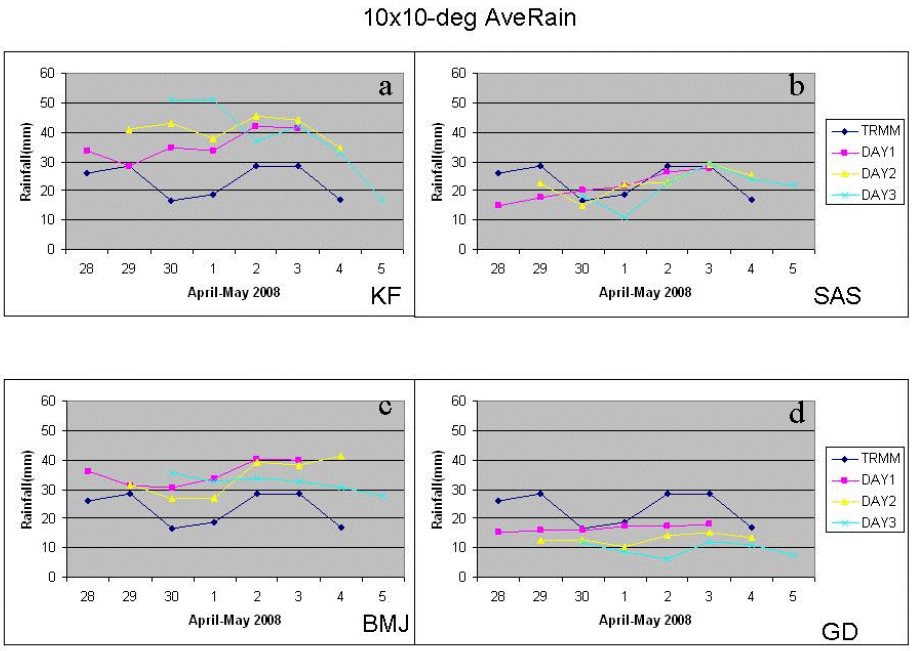

Fig. 19 Similar to Fig. 17, but for Nargis.

In general, it can be stated that KF produces the strongest intensity and GD features the weakest intensity. The experiments using SAS and BMJ feature intermediate intensification. Similarly KF produces the highest amount of associated rainfall and convective organisation while GD produces the least rainfall amount failing to capture the cyclone evolution and intensification. GD produces only a broad, diffused and a weak cyclone structure. As a result GD produces only the rainfall in the feeder bands to the south of the cyclone position. Also it can be noted that for the cases with weaker synoptic forcings, like that of Gonu, there is large difference in the behaviour of the cumulus parameterization schemes as well as its feedbacks with the surrounding environment. In contrast, for the cases with strong synoptic forcings as provided by the driving global model - like the case of Nargis - the performances of the various deep convection schemes are more or less similar.

This is in agreement with the observations by Yang and Tung (2003) that for the cases with strong synoptic forcings, the synoptic or mesoscale environment provides the primary control on the model's rainfall forecast skill, and the CPS schemes used in the model only slightly modify forecasts.

4.3 Tropical cyclone characteristics

The three systems under study have different history and characteristics and the peak intensity of the forecasts and the mature stages of its development vary from case to case. Ma and Tan (2009) assess the performance of various CPS schemes in the simulation of TCs and find some limitations identified in the distribution and intensity of precipitation and the partition into grid-resolvable and subgrid scale components. They found that the location and intensity are extremely sensitive to the choice of the cumulus convection. In their study, BMJ tends to overestimate the rainfall coverage and make false alarm of intense rainfall while KF gives the best simulation of TC on the 15Km grids. Grell's scheme tended to underestimate subgrid scale rainfall due to its deficiency in removing instability.

An effort has been made to diagnose the relatively large-scale structure of the TCs, by taking vertical cross section of the relative humidity (%) around the estimated centre of the system at the forecast time of the maximum intense or mature stage of development as simulated by the experiments (Panel (a-d) in figures 20, 22 and 24 for the four deep convective schemes KF, SAS, BMJ and GD respectively). Also the horizontal extent of relative humidity (RH - percentage), temperature (degrees Kelvin) and vertical velocity (hecto Pascal per second) in the 10x10 degree box surrounding the estimated centre locations in the forecasts corresponding to the four deep convective schemes are also shown in panels (e-h), (i-l) and (m-p) respectively. The circulation vectors shown in the figures are those corresponding to the vertical or horizontal planes, as the case is. The Figures 20, 22 and 24 correspond to the values at 00z of 06 June 2007 (day-3 forecast), 14 November 2007 and 02 May 2008 (day-2 forecasts each) respectively. In the case of Gonu experiments, as the system is not properly captured in intensity and location in the ICs, the maximum intensification takes place in a relatively longer time period and corresponds to the day-3 forecast from the initial condition of 03 June 2007. Otherwise for Sidr and Nargis cases, day-

2 forecasts are taken for the detailed analysis. Also figures 21, 23 and 25 show the distribution of total precipitation (APCPSFC) and non-convective part (NCPCPSFC) corresponding to the four deep convective schemes in panels (a-d).

For the case of cyclone Gonu, it can be broadly stated that none of the schemes produced observed peak intensity. However when compared with the vertical extent of the strong updraft and the humid air into the upper troposphere, KF outscores all other schemes with a stronger updraft near the cyclonic centre spreading over in the upper levels in the shape of a funnel and with a relatively dry middle troposphere. When comparing the distribution of RH at 850 hPa level, KF shows maximum vertical organization with the same initial and boundary conditions, whereas all other schemes produce relatively shallow humid layer spreading over more horizontal extent (particularly with GD the humid layer being very thin in the lower layers). From this distribution of RH along with the distribution of the rainfall for Gonu (Fig. 21), it can be easily assumed that KF and SAS produced the maximum convective organization and hence the humidity in the lower troposphere produced significant rainfall associated with the system by the day-3 forecast corresponding to 06 June 2007, compared to BMJ and GD with its weaker convective organization.

Temperature and vertical velocity distribution fields are also very weak for Gonu with predominantly cooler and lesser areas of upward motions. KF produced a narrow region of updraft near the centre with stronger downdrafts dominating the surroundings, where as GD shows predominantly weaker updraft and downdrafts cells spread over the box. From Fig. 21, it can be seen that only KF produces a component of non-convective rainfall whereas SAS generates almost entire amount of its rainfall from the deep convective scheme, though the day-3 forecast showed the least westward movement for KF. Generally intensity forecasts for all fields produced for Gonu by all the deep convective schemes are weaker compared to Sidr and Nargis. This is evident from figures 22-25 for Sidr and Nargis systems, where the vertical extent of high humid column is upto upper troposphere for KF and SAS, while GD shows the least vertical build up of moisture with maximum lateral spreading of the latent energy distribution restricted within a layer of 700 hPa. Generally KF showed maximum organization, stronger updrafts and downdrafts and precipitation, and GD showed the least organization and precipitation with the smaller cells of weaker vertical air motions

filled over the entire box which is apparently dissipating the total energy over the domain. These differences may be mainly coming from the characteristics of the deep convective parameterization schemes used for the forecast runs and its interaction with the other model physics components.

For Sidr and Nargis cases (Figs. 23 & 25), only KF and SAS produced some component of grid-scale rainfall, whereas BMJ and GD produced no significant amount of the same for any of the three cases. This implies that, at this resolution for tropical cyclone cases, the moisture processes in BMJ and GD parameterization schemes behave in a manner so that almost the entire precipitation is produced by the subgrid-scale. For KF, and under strong synoptic conditions for SAS also, the deep convection scheme leaves the grid points more moist, which may leads to super saturation at the grid points and which in turn eventually rains out as the large scale precipitation. The vertical cross section of relative humidity in figures 20, 22 and 24 also throws some light on the differences in the behaviour of the CPS schemes with respect to different synoptic environments associated with the three cases. KF always tends to have strong vertical updraft near the centre and invariably renders higher and higher levels moist, causing more grid scale condensation even in the case of Gonu. SAS could not produce any moist updraft which might have resulted into insignificant grid scale rain in the case of Gonu, while for Sidr and Nargis it did produce some grid-scale component. For BMJ and GD, virtually there is no vertical mixing and hence produced very shallow layers of moist air resulting into lesser contribution from the non-convective part. Other major difference in the behaviour of CPS schemes across all the cases is the apparent single tower-like structure of humidity build-up for KF in contrast to double tower structure on the either side of the centre for BMJ. SAS shows a combination of both varying with case-to-case, and GD shows no organized build-up. Generally it can be observed from the horizontal distributions that the concentrations of convective activity is to the northeast, south and southwest of cyclonic centre for Gonu, Sidr and Nargis respectively, which are generally in the opposite direction with respect to the movement of the system.

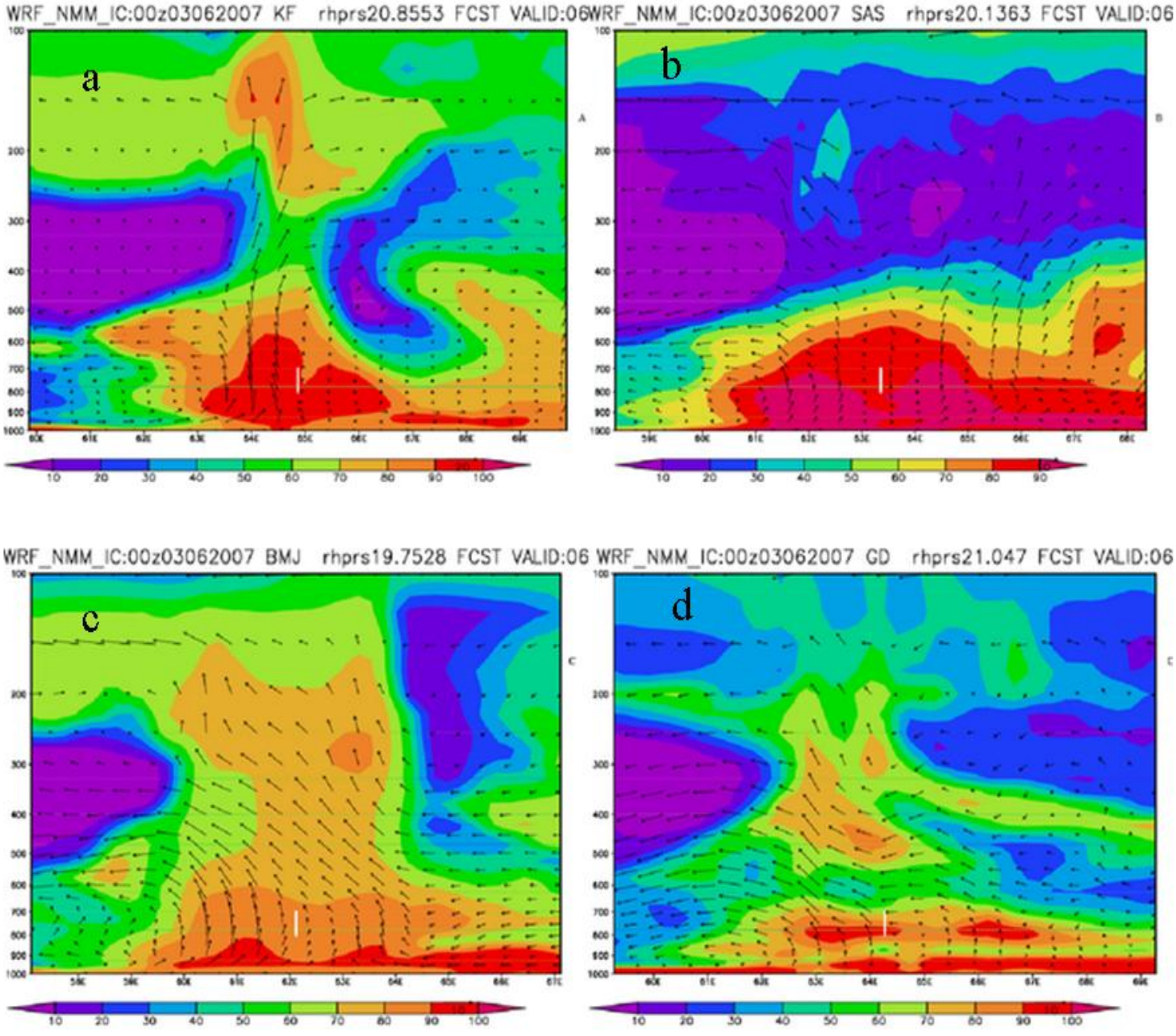
WRF_NMM_IC:00z03062007 KF rhprs20.8553 FCST VALID:06
a
WRF_NMM_IC:00z03062007 SAS rhprs20.1363 FCST VALID:06
b
WRF_NMM_IC:00z03062007 BMJ rhprs19.7528 FCST VALID:06
c
WRF_NMM_IC:00z03062007 GD rhprs21.047 FCST VALID:06
d

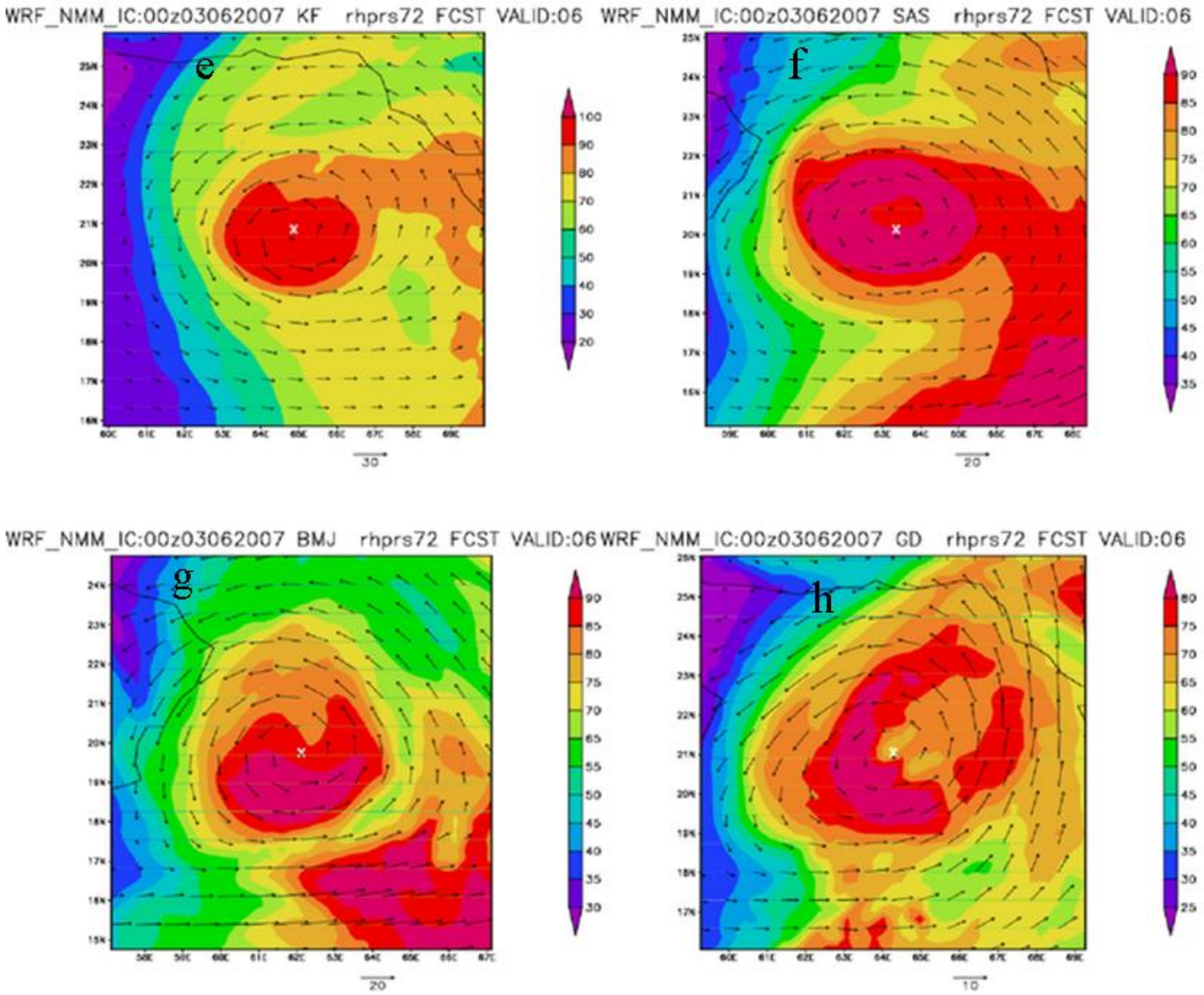
WRF_NMM_IC:00z03062007 KF rhprs72 FCST VALID:06
e
WRF_NMM_IC:00z03062007 SAS rhprs72 FCST VALID:06
f
WRF_NMM_IC:00z03062007 BMJ rhprs72 FCST VALID:06
g
WRF_NMM_IC:00z03062007 GD rhprs72 FCST VALID:06
h

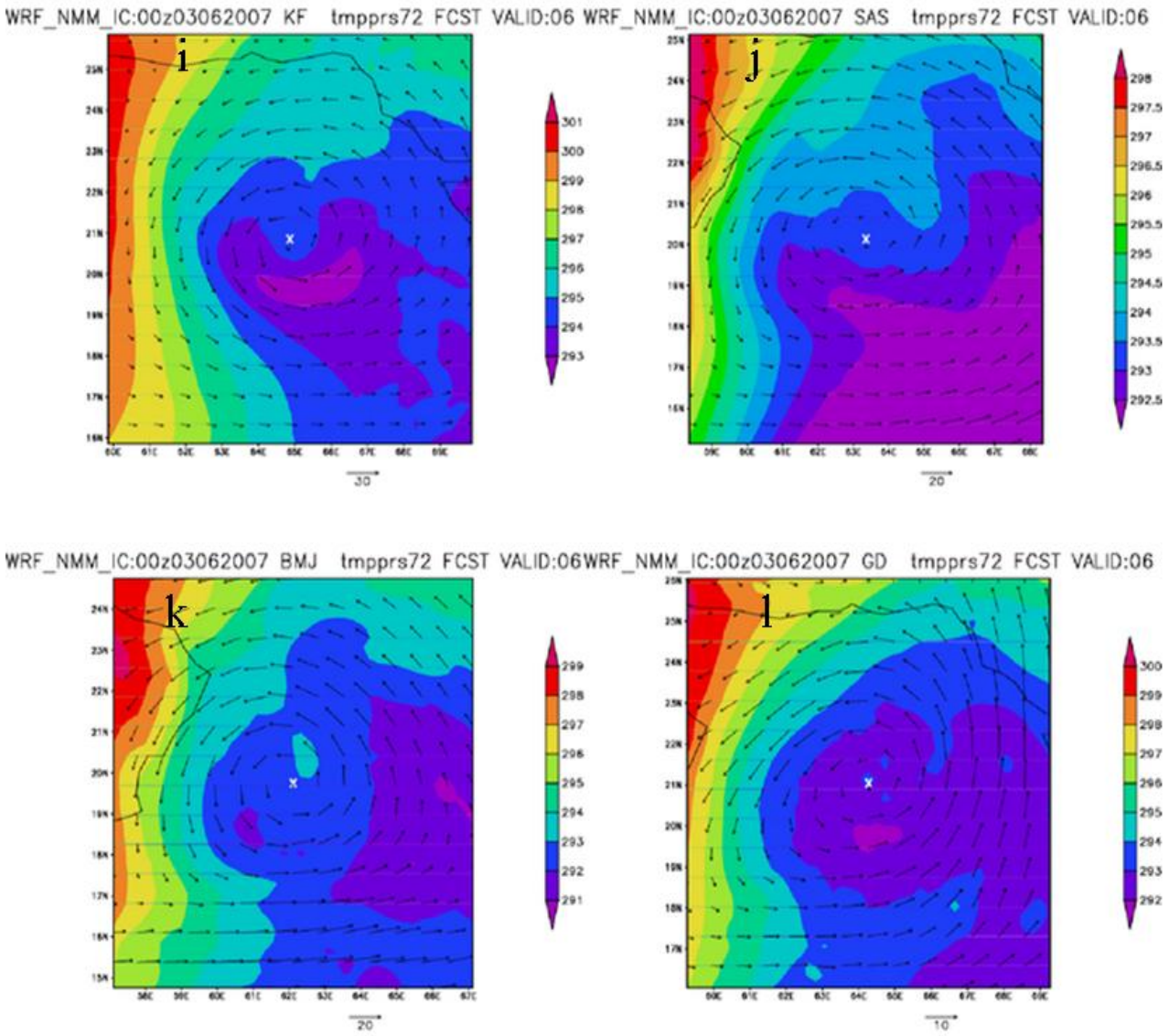
WRF_NMM_IC:00z03062007 KF tmpprs72 FCST VALID:06
i
WRF_NMM_IC:00z03062007 SAS tmpprs72 FCST VALID:06
j
WRF_NMM_IC:00z03062007 BMJ tmpprs72 FCST VALID:06
k
WRF_NMM_IC:00z03062007 GD tmpprs72 FCST VALID:06
l

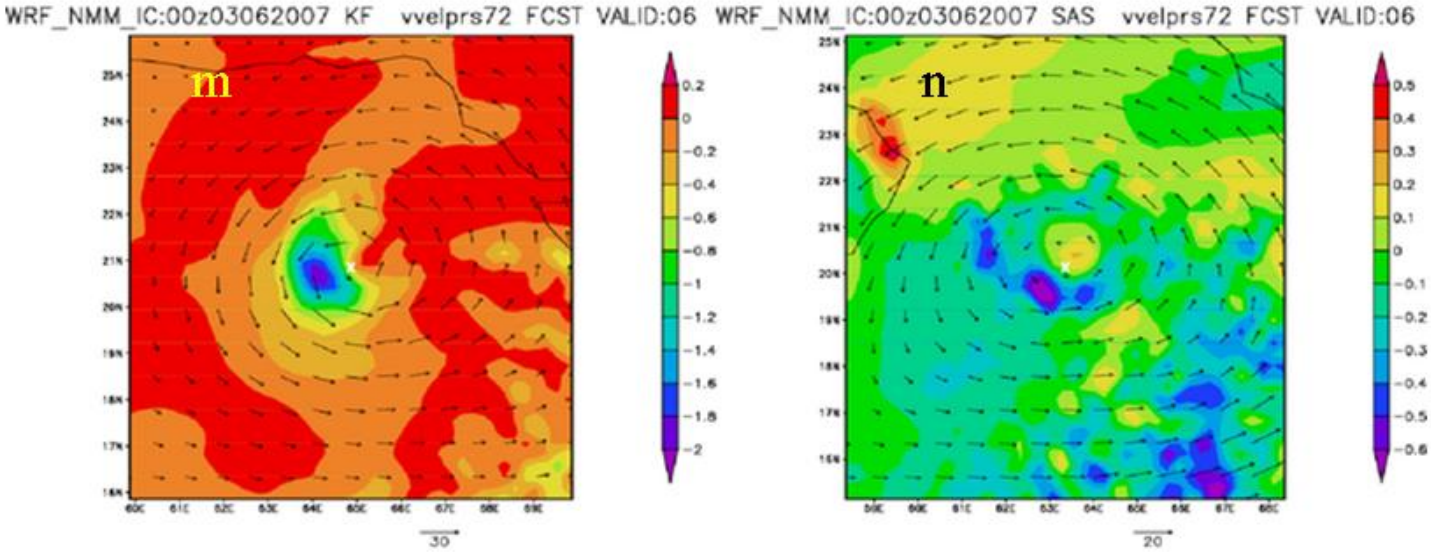
WRF_NMM_IC:00z03062007 KF vvelprs72 FCST VALID:06
m
WRF_NMM_IC:00z03062007 SAS vvelprs72 FCST VALID:06
n

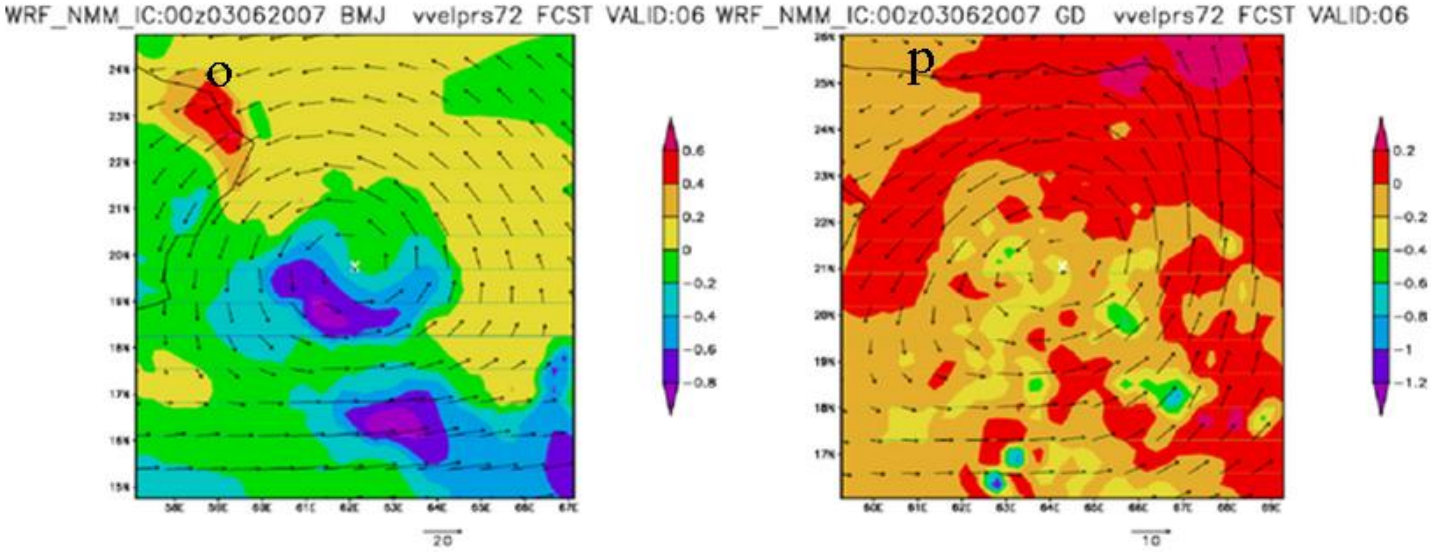
WRF_NMM_IC:00z03062007 BMJ vvelprs72 FCST VALID:06
o
WRF_NMM_IC:00z03062007 GD vvelprs72 FCST VALID:06
p

Fig. 20 Panels (a-d) are the vertical cross sections of relative humidity (%age - shaded) along the predicted TC centre by WRF NMM models along with vertical wind vectors (m/s) for four CPS schemes. Panels (e-f) are the corresponding geographical distribution of relative humidity (%age - shaded) at 850 hPa level in the grid box around the predicted locations of TC with four CPS schemes along with the horizontal wind vectors (m/s). Panels (i-k) are similar to (e-h), but for temperature (K) at 850 hPa level and panels (m-p) is for omega (hPa/s). All are valid for day-3 forecasts at 00Z 06 June, 2007.

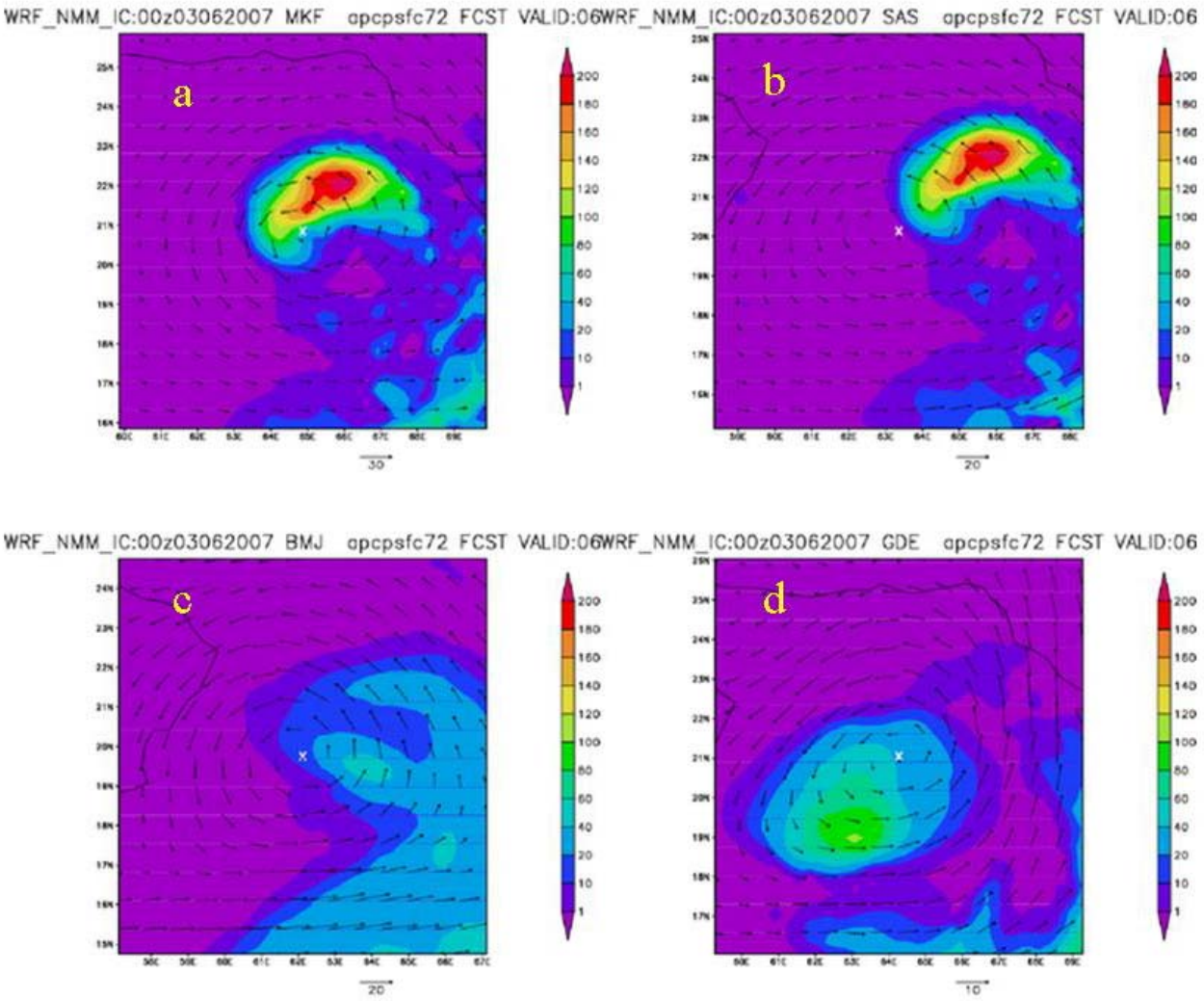

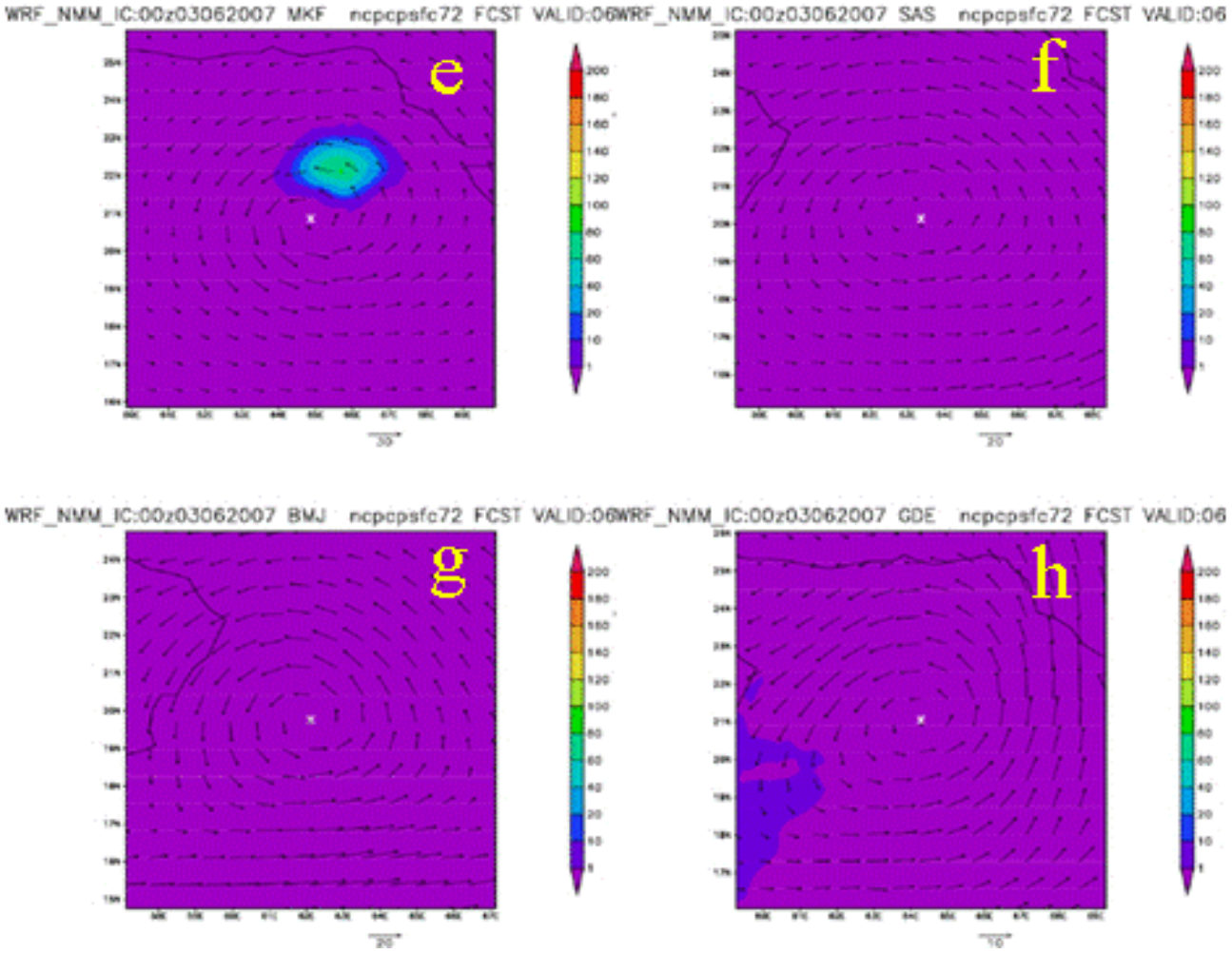

Fig. 21 Total precipitation (mm/day) and non-convective precipitation (mm/day) for the box areas corresponding to the predicted centres of TCs by WRF NMM with four CPS schemes (a-d and e-h respectively) valid for day-3 forecasts at 00Z 06 June, 2007.

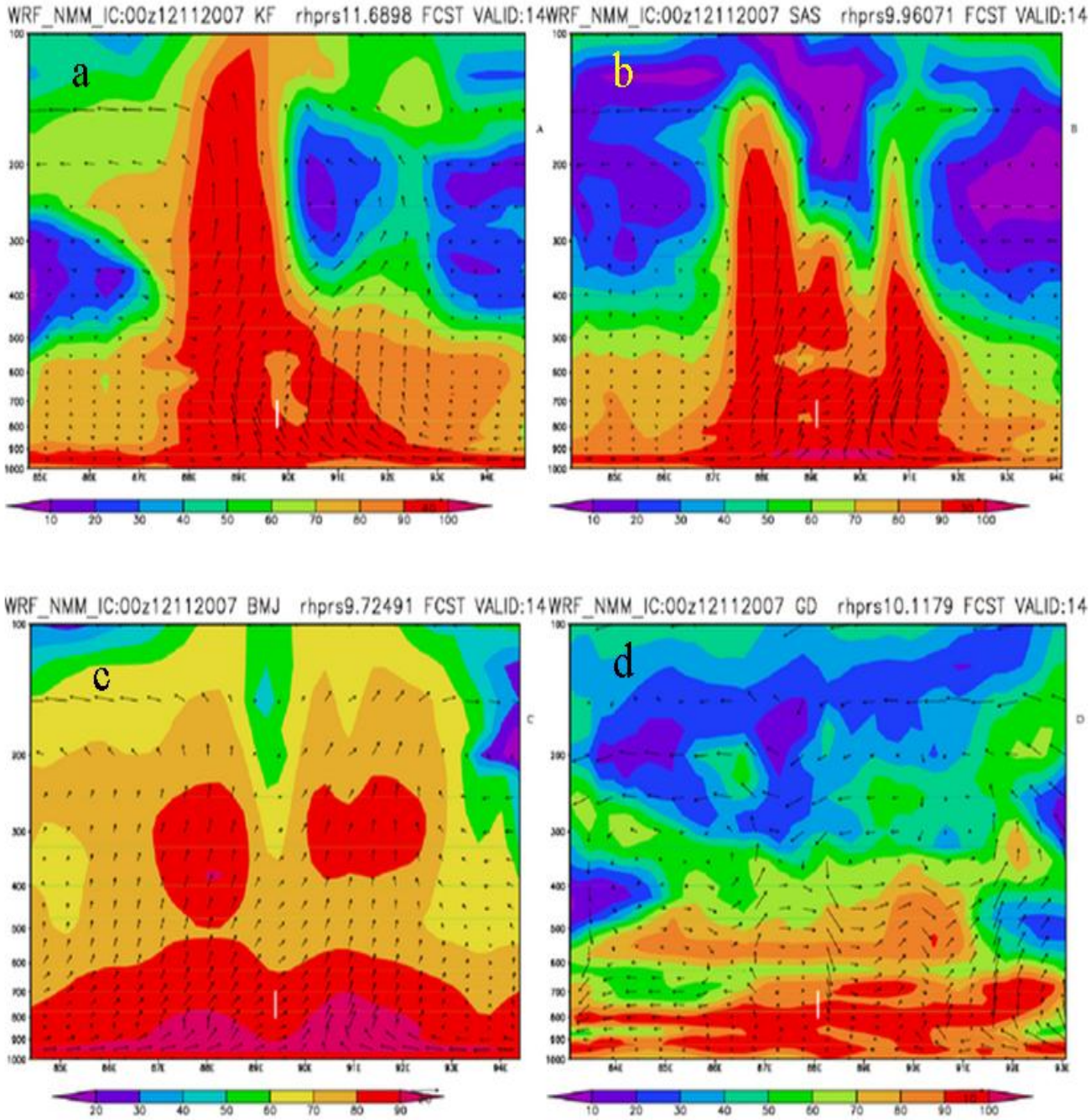
WRF_NMM_IC:00z12112007 KF rhprs11.6898 FCST VALID:14
a
WRF_NMM_IC:00z12112007 SAS rhprs9.96071 FCST VALID:14
b
WRF_NMM_IC:00z12112007 BMJ rhprs9.72491 FCST VALID:14
c
WRF_NMM_IC:00z12112007 GD rhprs10.1179 FCST VALID:14
d

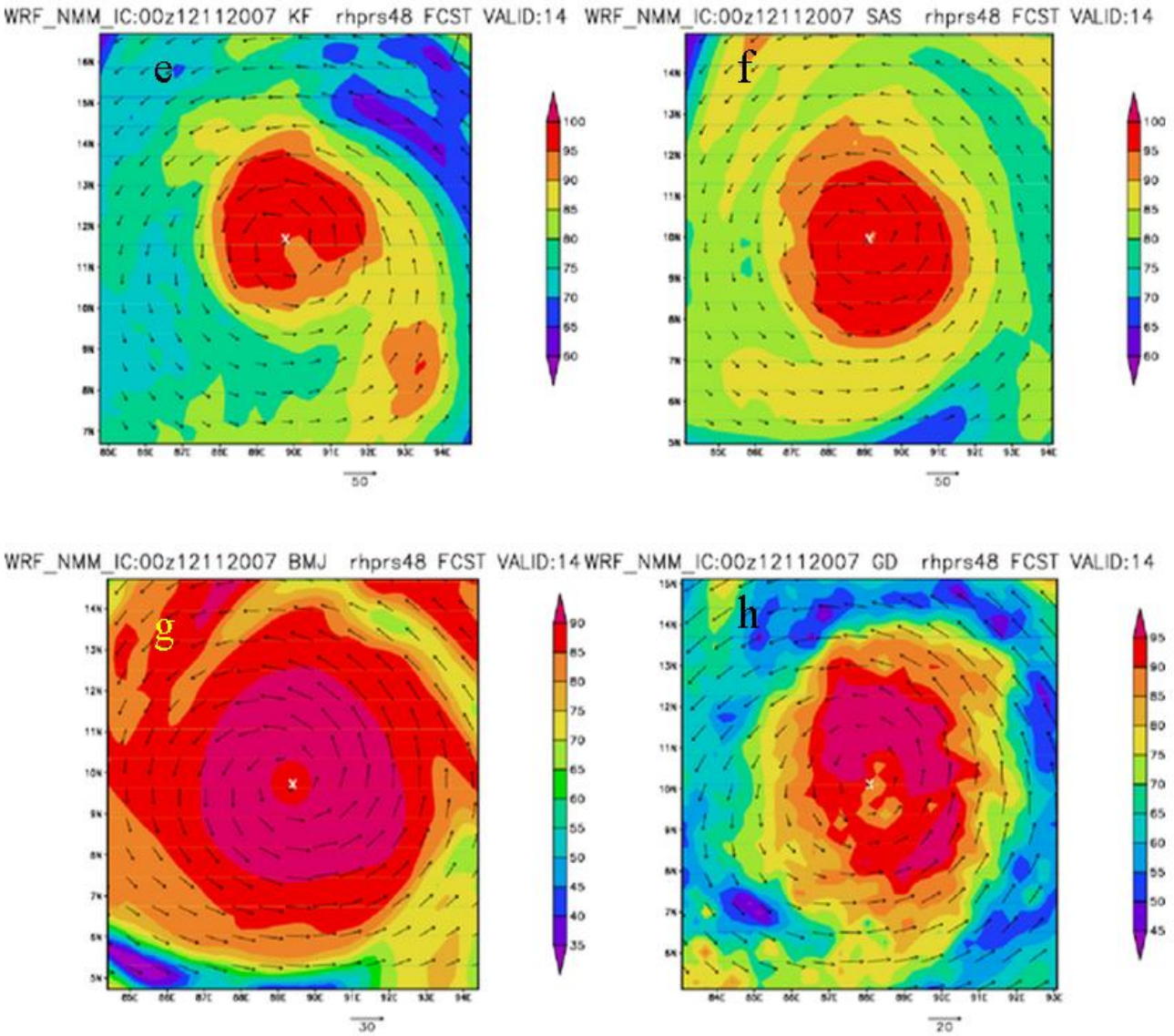
WRF_NMM_IC:00z12112007 KF rhprs48 FCST VALID:14
e
WRF_NMM_IC:00z12112007 SAS rhprs48 FCST VALID:14
f
WRF_NMM_IC:00z12112007 BMJ rhprs48 FCST VALID:14
g
WRF_NMM_IC:00z12112007 GD rhprs48 FCST VALID:14
h

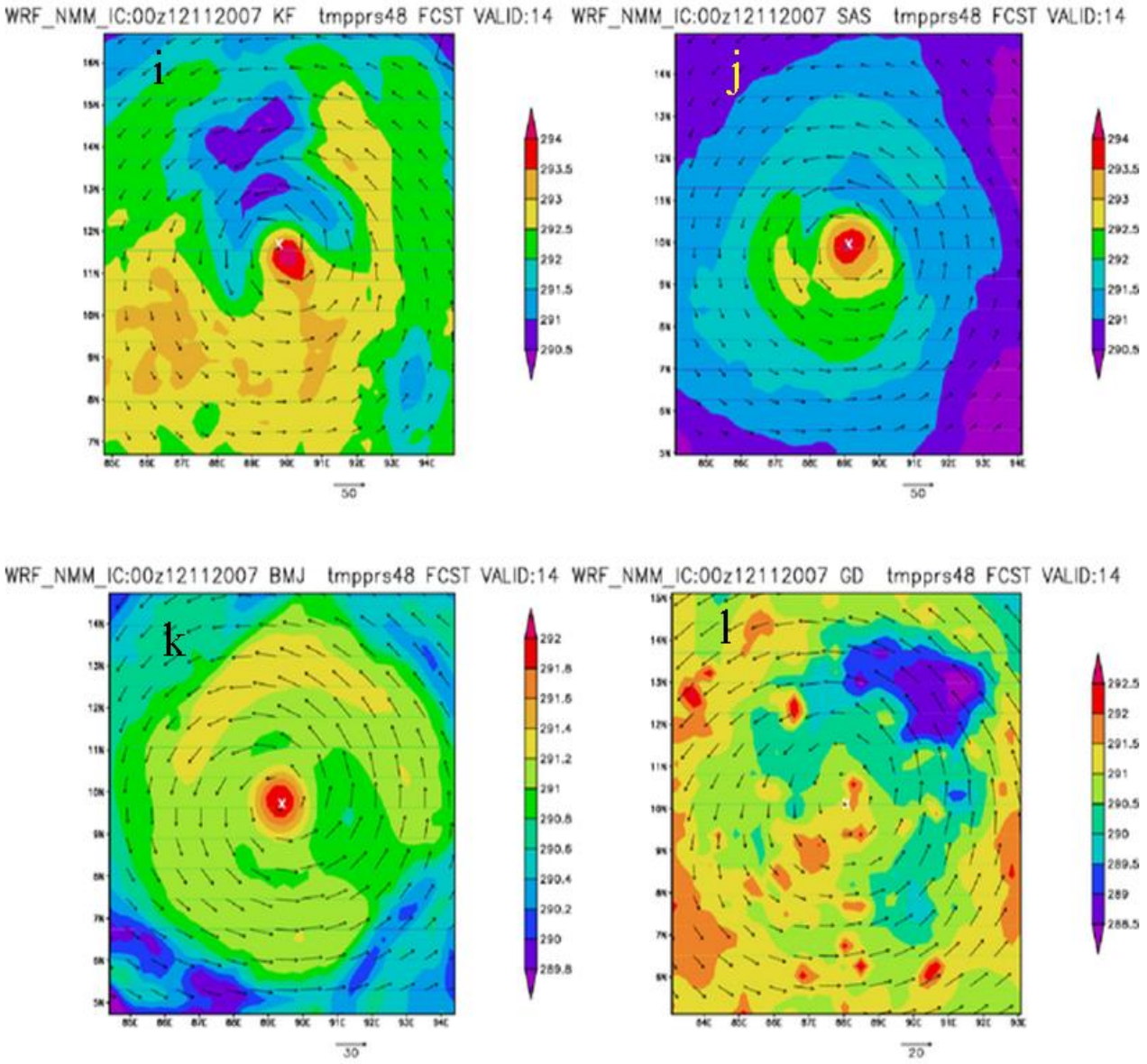
WRF_NMM_IC:00z12112007 KF tmpprs48 FCST VALID:14
i
294
293.5
293
292.5
292
291.5
291
290.5
WRF_NMM_IC:00z12112007 SAS tmpprs48 FCST VALID:14
j
294
293.5
293
292.5
292
291.5
291
290.5
WRF_NMM_IC:00z12112007 BMJ tmpprs48 FCST VALID:14
k
292
291.8
291.6
291.4
291.2
291
290.8
290.6
290.4
290.2
290
289.8
WRF_NMM_IC:00z12112007 GD tmpprs48 FCST VALID:14
l
292.5
292
291.5
291
290.5
290
289.5
289
288.5

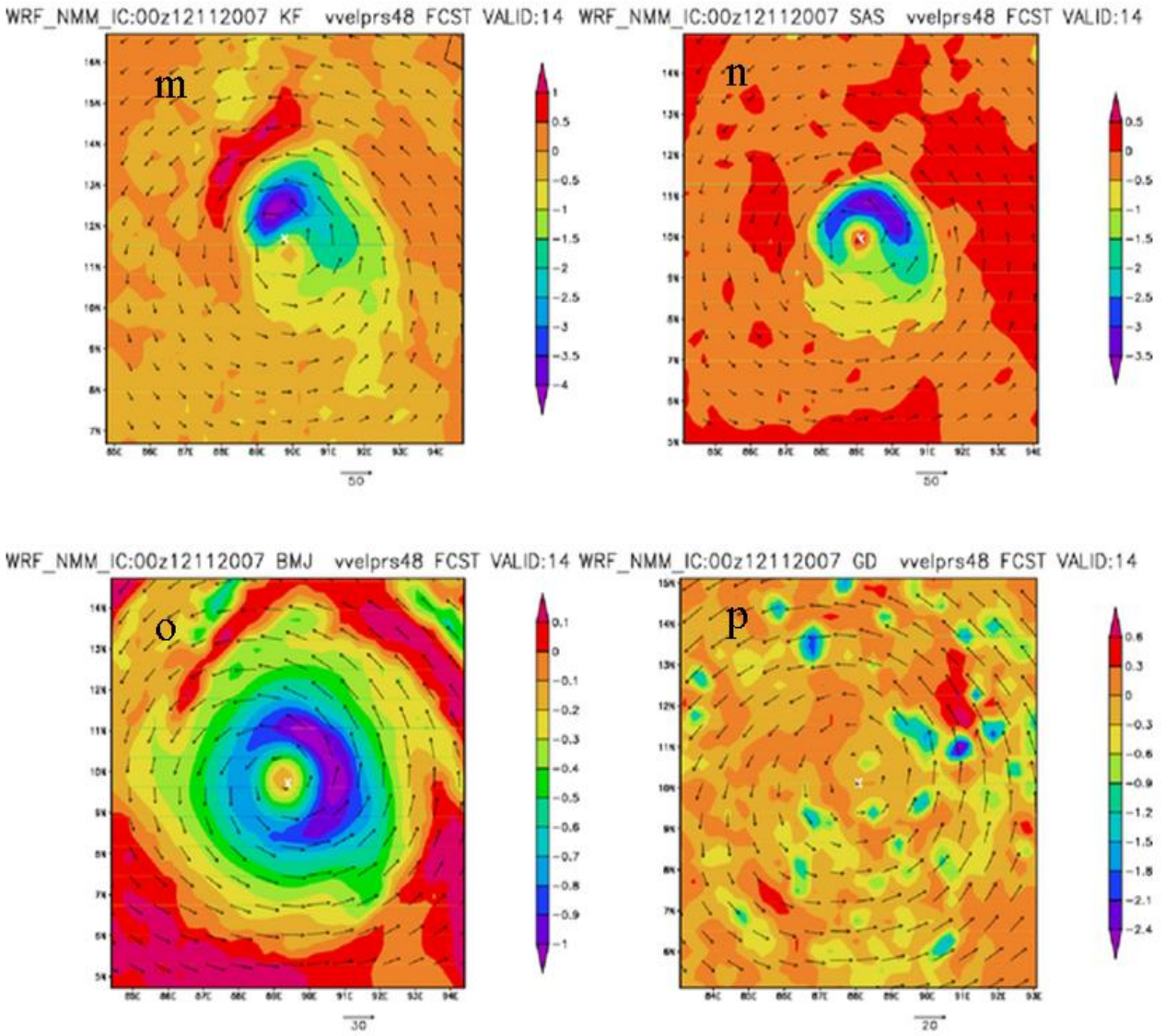

Fig. 22 Similar to Fig.20, but valid for day-2 forecasts at 00Z 14 November, 2007.

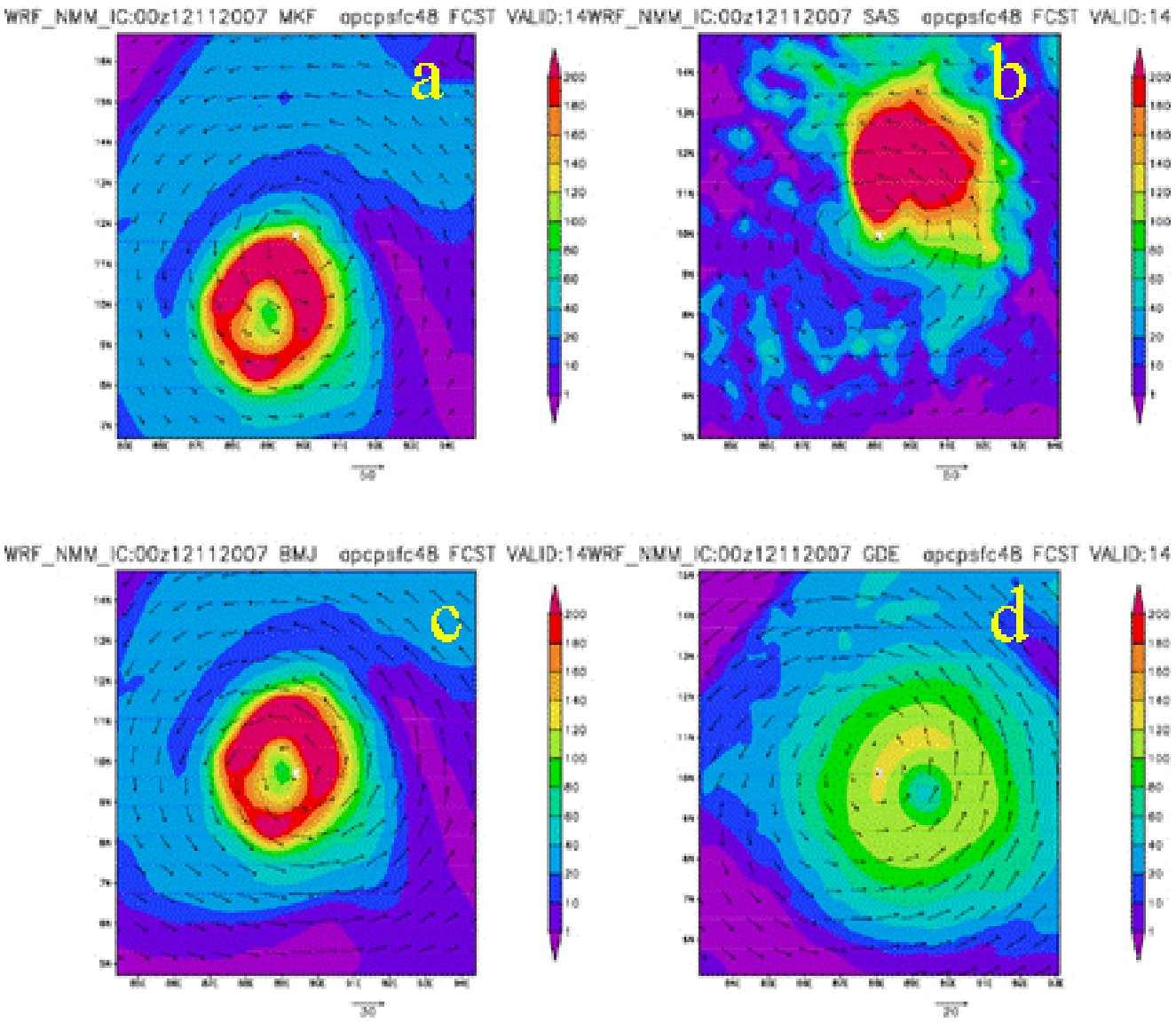
WRF_NMM_IC:00z12112007 MKF apcpsfc48 FCST VALID:14WRF_NMM_IC:00z12112007 SAS apcpsfc48 FCST VALID:14
a
b
WRF_NMM_IC:00z12112007 BMJ apcpsfc48 FCST VALID:14WRF_NMM_IC:00z12112007 GDE apcpsfc48 FCST VALID:14
c
d

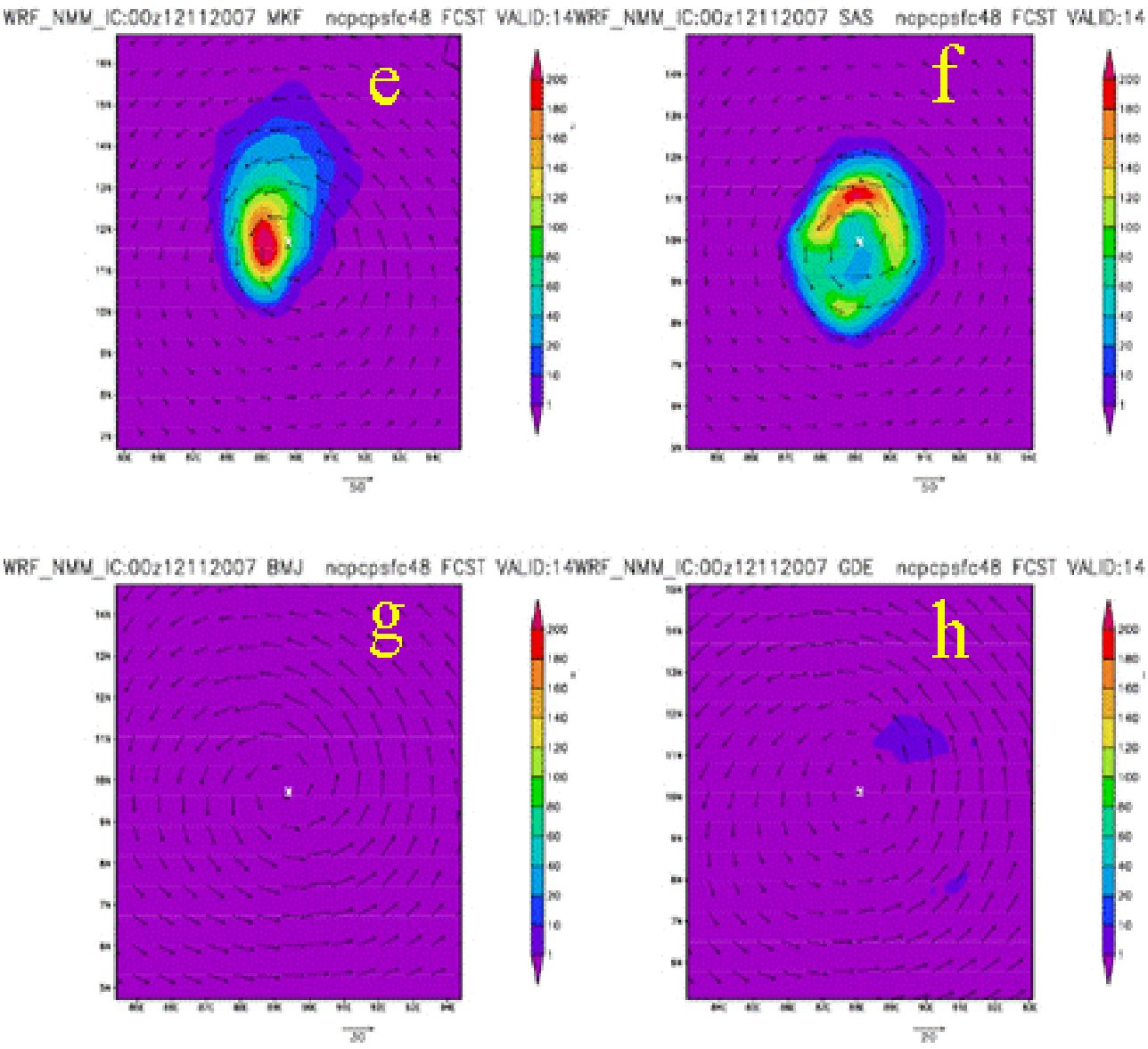

Fig. 23 Similar to Fig. 21, but for day-2 forecasts at 00Z 14 November, 2007.

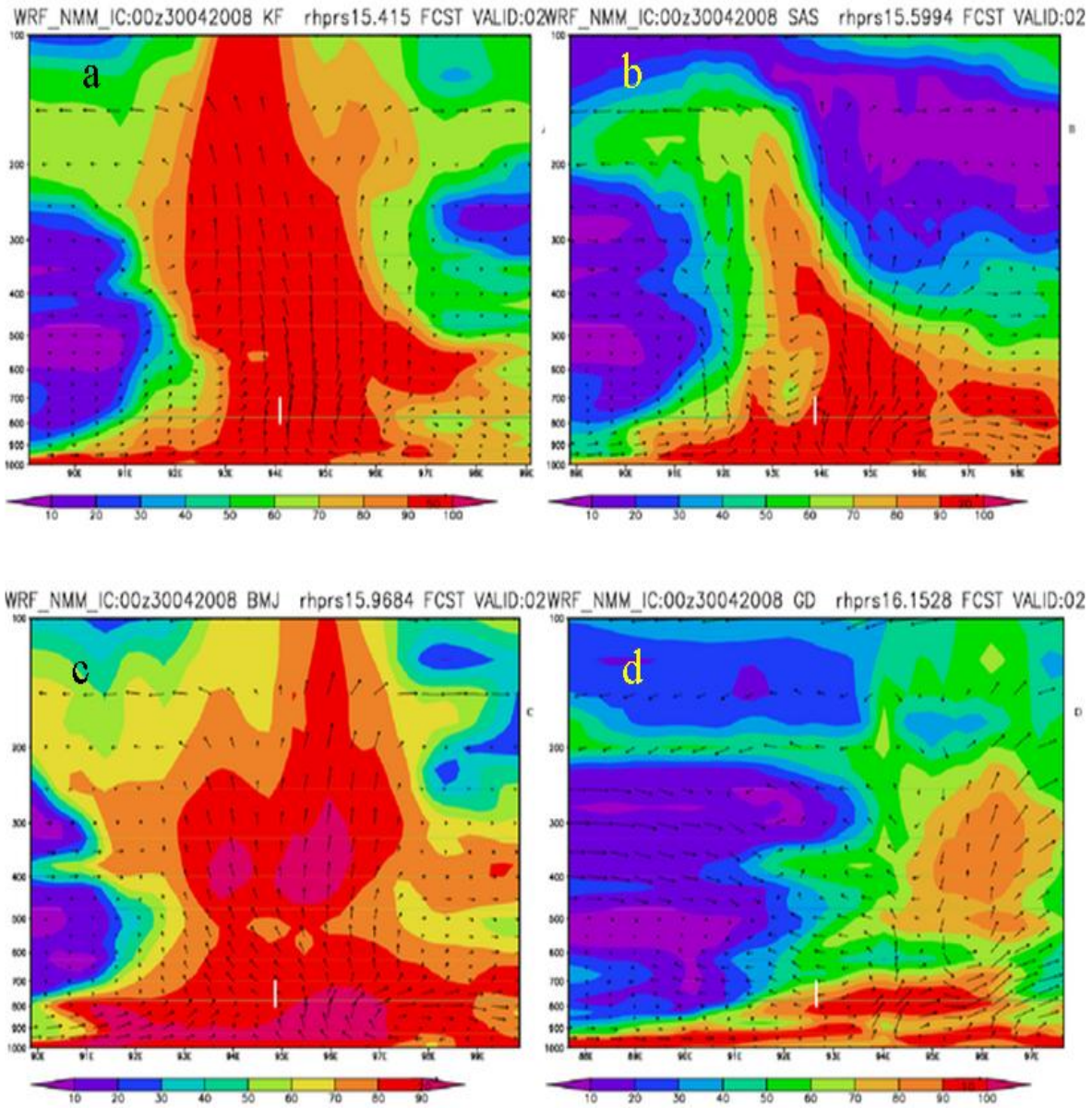
WRF_NMM_IC:00z30042008 KF rhprs15.415 FCST VALID:02
WRF_NMM_IC:00z30042008 SAS rhprs15.5994 FCST VALID:02
WRF_NMM_IC:00z30042008 BMJ rhprs15.9684 FCST VALID:02
WRF_NMM_IC:00z30042008 GD rhprs16.1528 FCST VALID:02
a
b
c
d

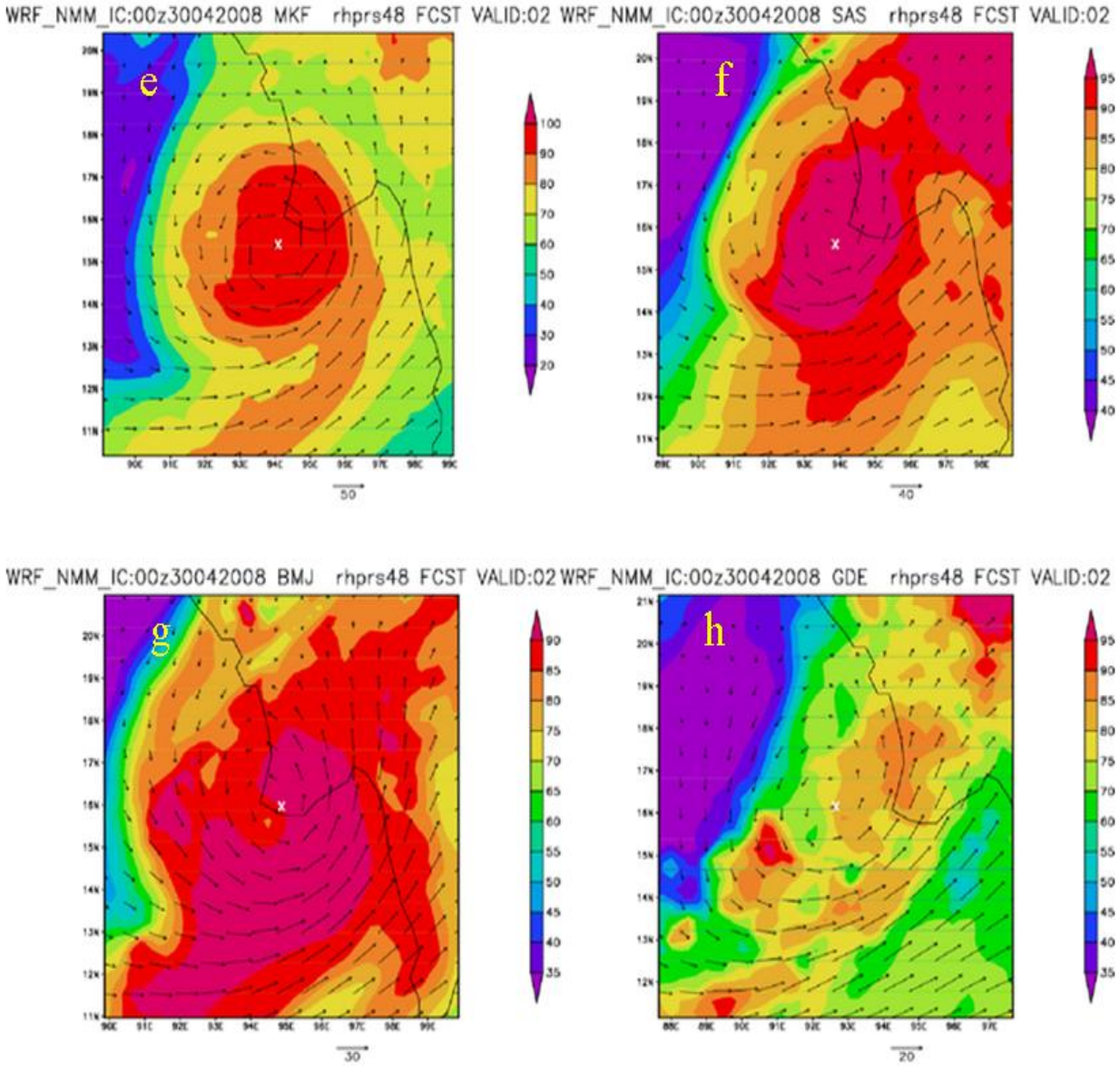
WRF_NMM_IC:00z30042008 MKF rhprs48 FCST VALID:02
e
WRF_NMM_IC:00z30042008 SAS rhprs48 FCST VALID:02
f
WRF_NMM_IC:00z30042008 BMJ rhprs48 FCST VALID:02
g
WRF_NMM_IC:00z30042008 GDE rhprs48 FCST VALID:02
h

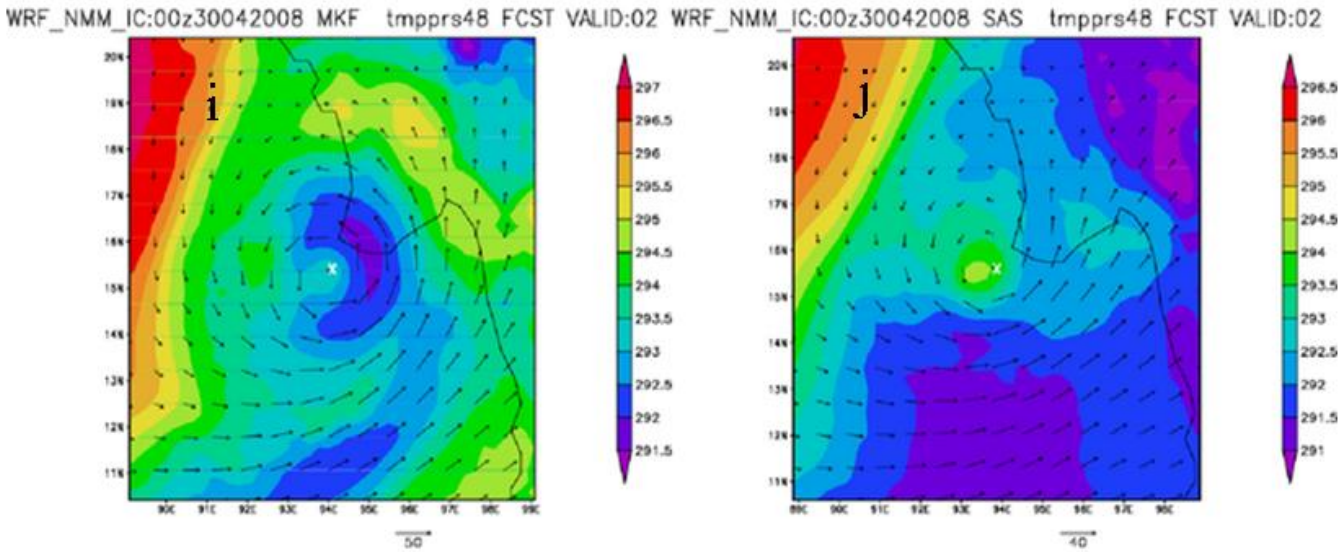
WRF_NMM_IC:00z30042008 MKF tmpprs48 FCST VALID:02
i
297
296.5
296
295.5
295
294.5
294
293.5
293
292.5
292
291.5
50
WRF_NMM_IC:00z30042008 SAS tmpprs48 FCST VALID:02
j
296.5
296
295.5
295
294.5
294
293.5
293
292.5
292
291.5
291
40

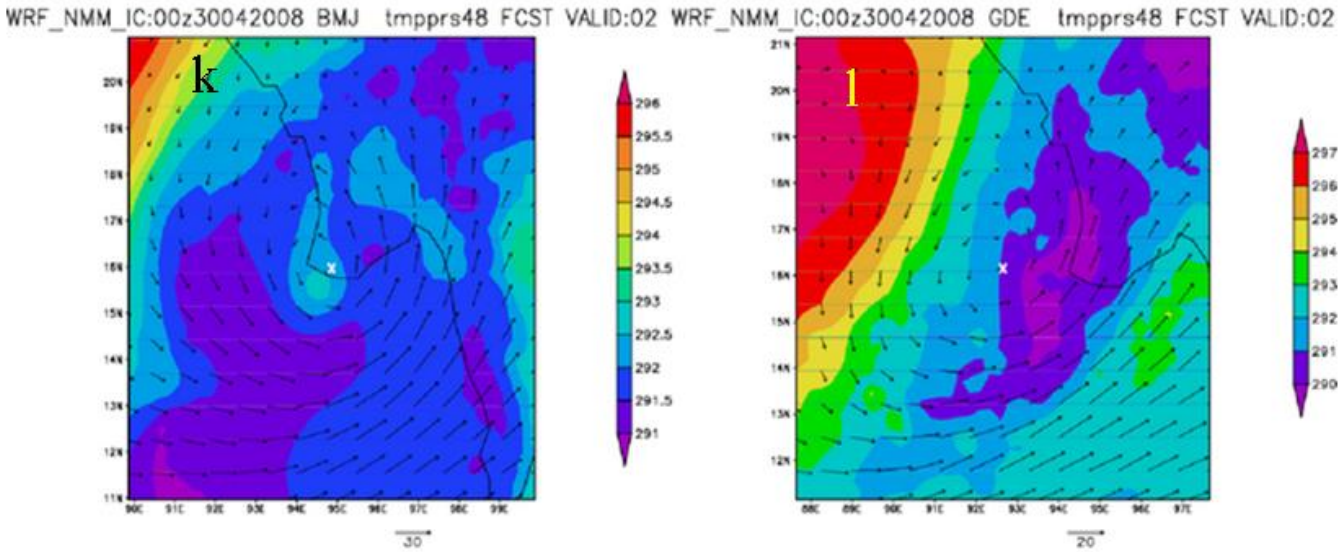
WRF_NMM_IC:00z30042008 BMJ tmpprs48 FCST VALID:02
k
296
295.5
295
294.5
294
293.5
293
292.5
292
291.5
291
30
WRF_NMM_IC:00z30042008 GDE tmpprs48 FCST VALID:02
l
297
296
295
294
293
292
291
290
20

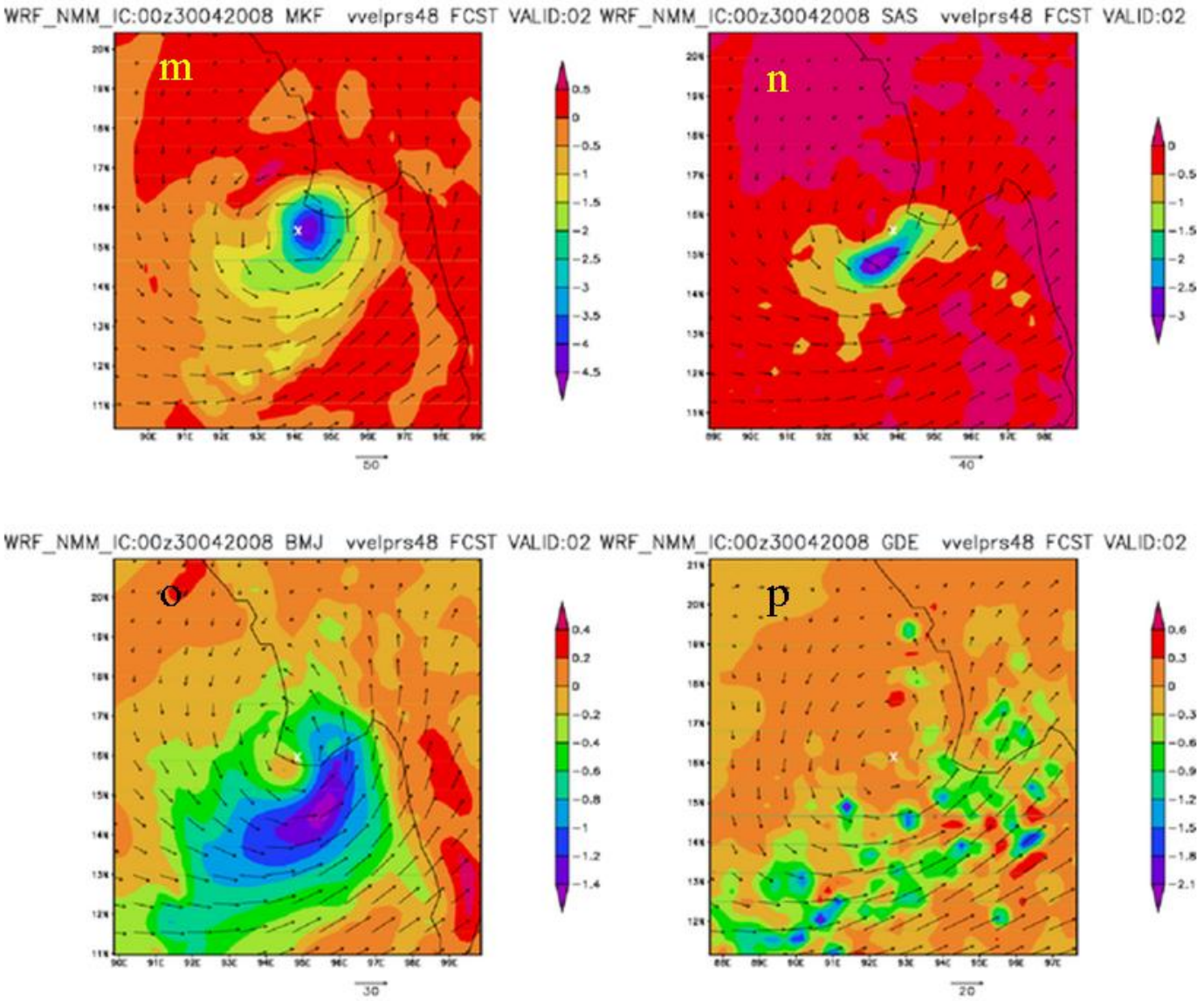

Fig. 24 Similar to Fig. 20, but for day-2 forecasts at 00Z 02 May, 2008.

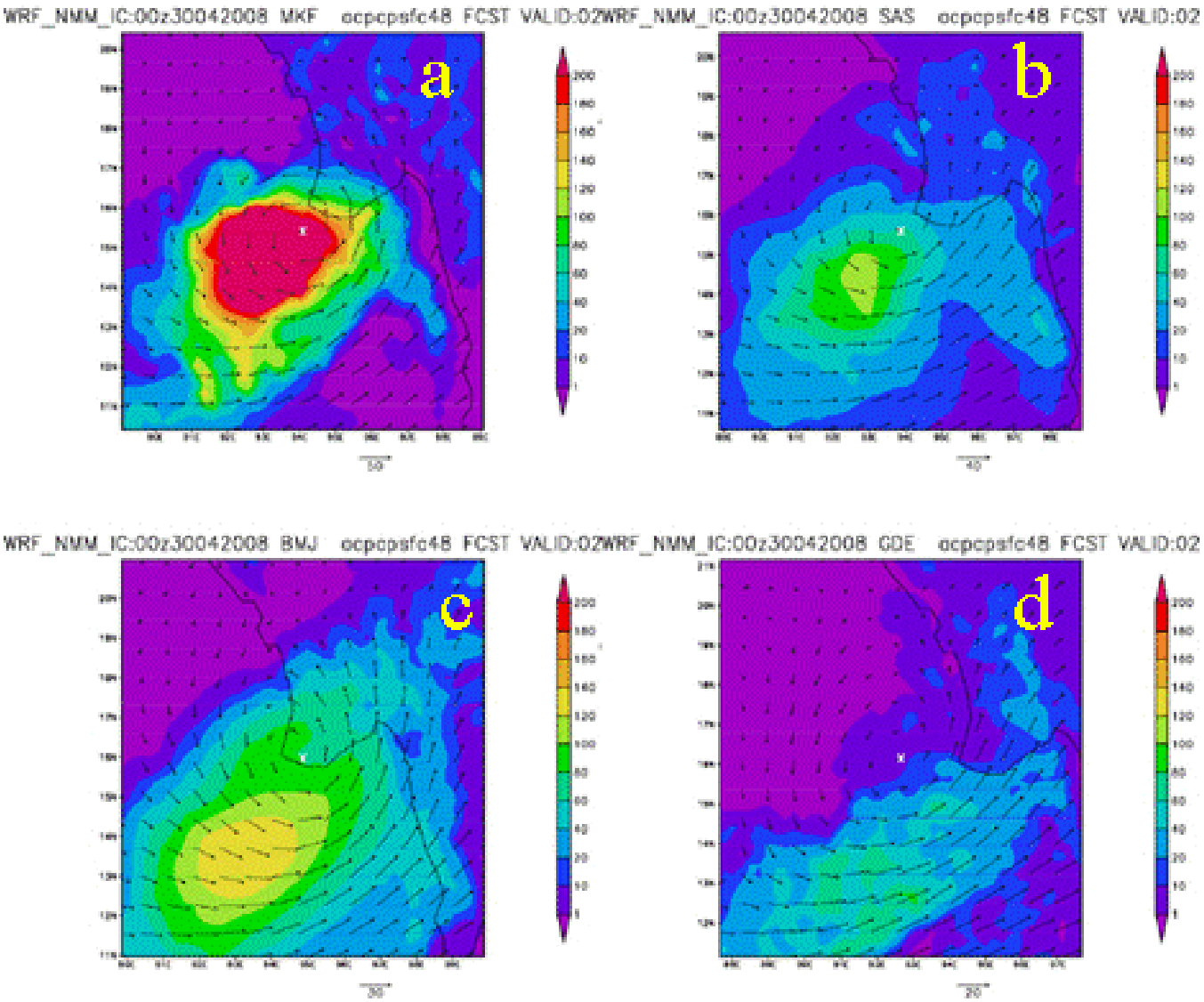
WRF_NMM_IC:00z30042008 MKF acpcpsfc48 FCST VALID:02
WRF_NMM_IC:00z30042008 SAS acpcpsfc48 FCST VALID:02
a
b
WRF_NMM_IC:00z30042008 BMJ acpcpsfc48 FCST VALID:02
WRF_NMM_IC:00z30042008 GDE acpcpsfc48 FCST VALID:02
c
d

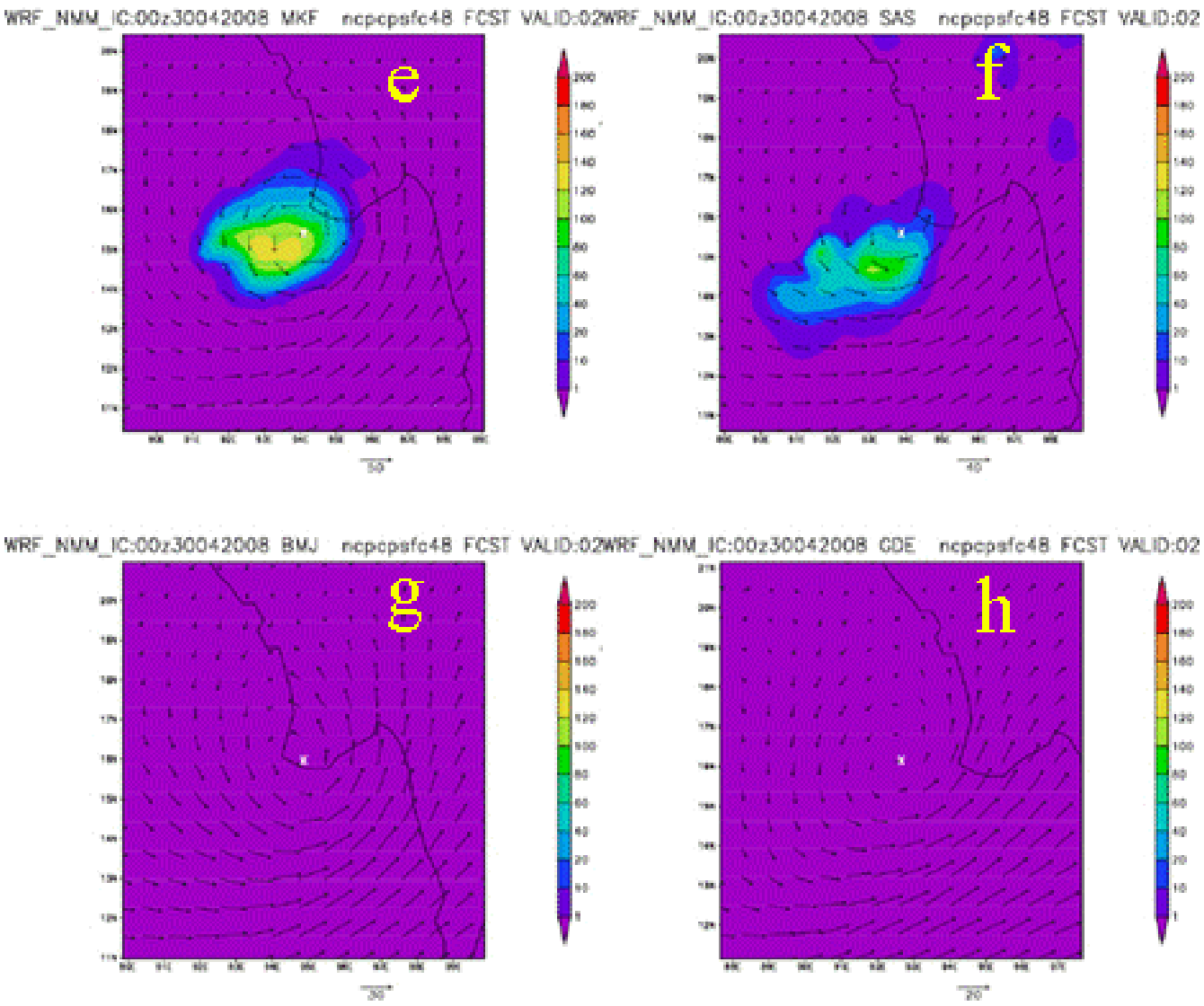

Fig. 25 Similar to Fig.21, but for day-2 forecasts at 00Z 02 May, 2008.

4.4 Standard rainfall verification scores

Bias scores (BS), threat scores (TS) and equitable threat scores (ETS) are some of the widely accepted standard parameters for model performance for the categorical measures like rainfall. The rainfall has been divided into 10 different thresholds varying from 0-10 cm at 1 cm interval. The verification is done against the TRMM rainfall over the box with the centre of the corresponding forecast run (Fig. 26) with panels a, c and e corresponding to the BS, TS and ETS respectively averaged across the three cases and b, d and f those averaged across all the four deep convective schemes. In the lower thresholds all the schemes equally over predict the total precipitation. KF shows consistently slightly higher bias score at around 1.5 at all thresholds and those for BMJ is more or less approaching near perfect value of 1 at higher thresholds (5cm and more). SAS is showing more and more over prediction at higher thresholds and GD produces more over prediction in the medium thresholds. At the same time, averaged across all deep convective schemes, Sidr produced in general over prediction of bias scores and Gonu under predicted the higher amount of rainfall. Averaged across all the physics, the model is able to produce a reasonably stable and accurate bias score for all the ranges of rainfall amount for Nargis case. When the TS and ETS scores are examined, there is not much difference between the deep convective parameterization schemes when averaged over all cases and the correspondence between the forecast “yes” events and observed “yes” events being only a fraction and decreasing as the threshold increases. Only for SAS there is a marginal increase in the ETS compared to other schemes in lower thresholds. However it can be noted that when averaged across all the deep convective schemes, Nargis scored significantly high in TS and ETS values and Gonu scored negative for ETS scores while the Sidr scored in between. So it can be easily drawn from these analyses that the mesoscale model forecasts are strongly influenced by the synoptic environment and the quality of input data as compared with the deep convective schemes.

The performance of the model at 24-hr, 48-hr and 72-hr forecasts are also separately analysed in figures (27-29) respectively. In general, at all thresholds, there is an increase in over prediction with the forecast length. For KF, day-1 forecast has near perfect value of 1 in all thresholds. SAS over predicts in all thresholds and BMJ under predicts at

higher thresholds while GD under predicts at medium thresholds. Day-3 forecasts give much more over prediction compared to day-1 and day-2 for all schemes especially KF and SAS. Averaged over all CPS schemes, Sidr gave over prediction at all forecast lead times. In Gonu case, there is more and more underprediction from lower to higher thresholds. This indicates that the model in general could not predict the heavy rainfall amounts associated with the TCs.

For Gonu it was earlier observed that the forecasts were very much out and the comparison of the rainfall values captured within the 10x10 degree box corresponding to the forecast positions of the system may not be very fair and hence the scores can be considered more or less unreliable. A more fair comparison is possible for Nargis case where it is consistently giving a reasonably better prediction at all thresholds and at all forecast lead times. TS scores averaged across all TC systems do not leave much to choose from. Averaged over all CPS schemes, Nargis scores fairly higher than Sidr and Gonu when averaged across all the model physics experiments with a value of nearly 0.70 at the lowest threshold at all the forecast lead times. In the case of ETS, SAS produced higher scores at all thresholds at day-3 and GD at day-1, though the general reliability of the forecast is very poor at less than 0.15 even at the lowest threshold. The sensitivity of the synoptic conditions to the reliable rainfall forecasts can not be again underestimated as it is shown that the ETS scores vary significantly between the three cases where Nargis gives consistently better and Gonu worse performances at all forecast lead times. Here also, the scores are less than 0.30 even at lowest threshold. Gonu performed worse with negative ETS at higher thresholds and at forecast days 2 and 3. Fig. 30 gives the detailed performance of each physics options for each individual cases averaged across all the forecast lead times of day-1 to day-3, where BS is higher for all the deep convective schemes for Sidr and TS and ETS scores are much better for Nargis irrespective of the deep convection schemes used. It can be noted that ETS scores are highest for GD in general for Nargis case and lowest for Gonu. However, GD is not consistently giving better results during the weak synoptic conditions (or for the more erroneous boundary conditions) like that of Gonu case, where ETS is negative for GD and all other schemes show no skill.

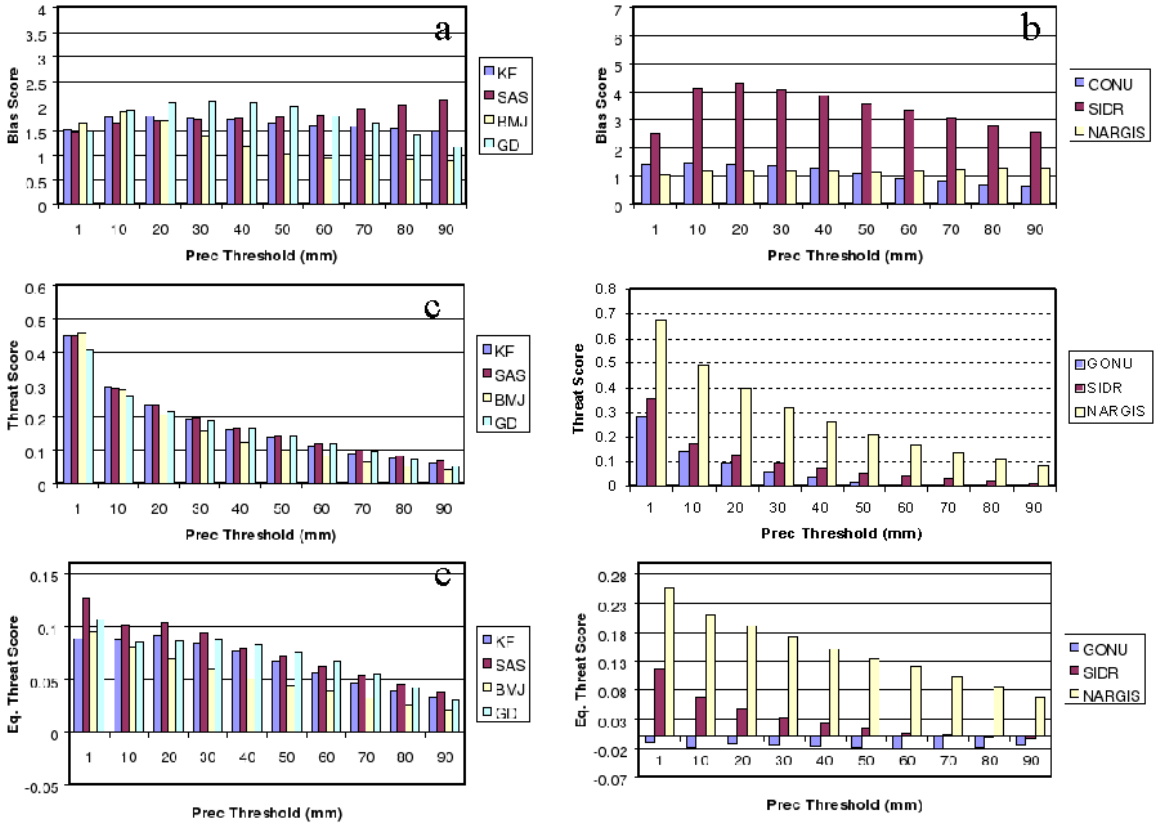

Fig. 26 Bias Score (BS), Threat Score (TS) and Equitable Threat Score (ETS) for total rainfall (mm/day) for thresholds 1, 10, 20… 90mm, averaged across all three TC cases (a, c, and e) and averaged across all CPS schemes (b, d and f).

The diagnosis of the reasons for these behaviour patterns of the deep convection schemes in the different scenarios requires much deeper analysis and sensitivity studies and is beyond the scope of this study. However one aspect of the so called cumulus parameterization problem lies in the representation of both resolved and sub grid-scale precipitation processes and its dependency on the model resolution (Frank, 1983). Wang and Seaman (1997) reported following a very detailed study that the rainfall partitioning into sub grid scale and grid scale is sensitive to the particular parameterization scheme chosen, but relatively insensitive to the model resolution as well as to the convective environments. Fig. 31 shows the percentage ratio of non-convective to total rainfall averaged for all forecast period along with the mean total daily precipitation averaged across all the cases as well as across all the physics experiments. It is evident that KF produced maximum total rainfall followed by BMJ, SAS and GD with GD producing only about one-third quantity of KF

rainfall amount as a whole. KF and SAS produced more fraction of precipitation of grid-scale to the total precipitation (10-14 %) whereas BMJ and GD produced very negligible fraction (upto about 2 %). It is to be noted that though there is not much difference between Sidr and Nargis in the total as well as the grid-scale fraction of precipitation, there seems to be a significant reduction in the total as well as the fractional rainfall production for Gonu.

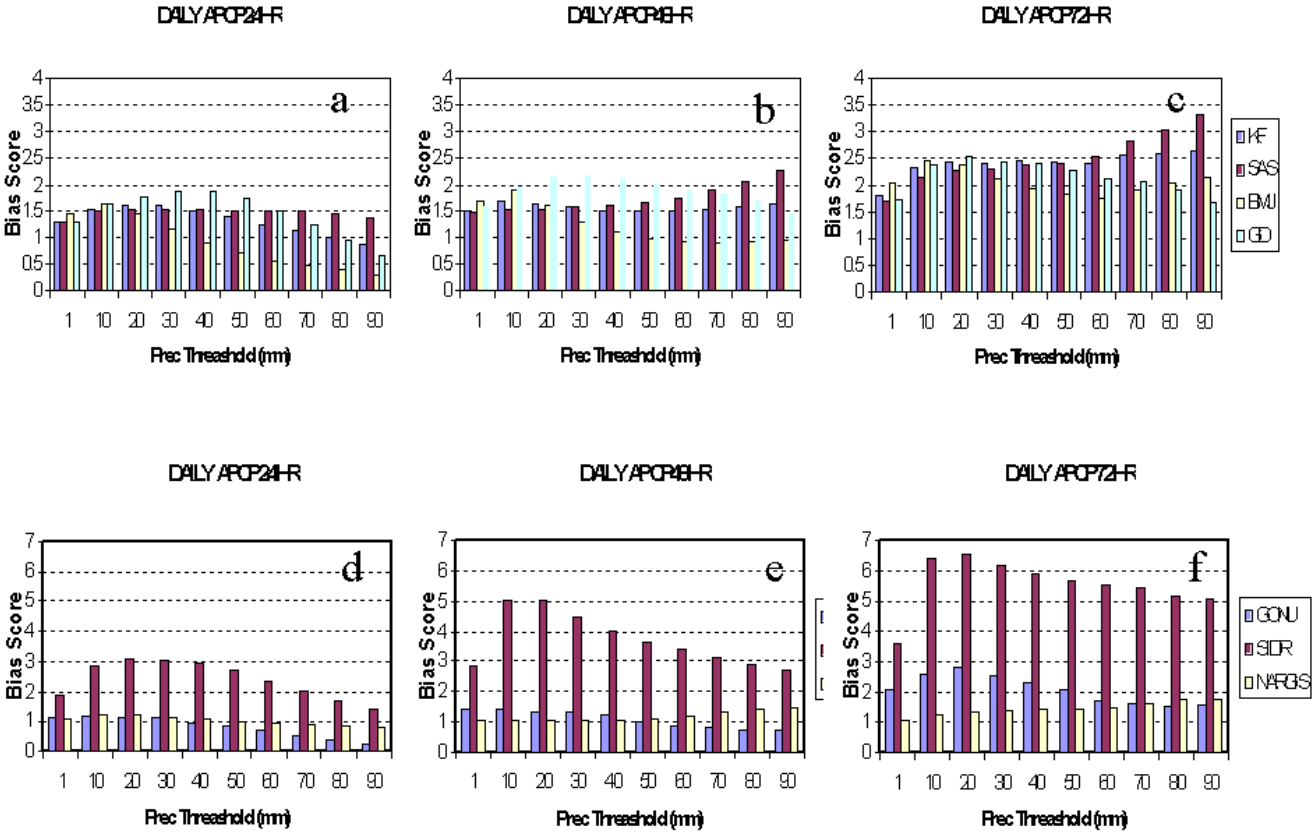

Fig. 27 Similar to Fig. 26, but only BS separately at forecast hours 24, 48 and 72 and averaged across all 3 cases (a-c) and averaged across all 4 CPS schemes (d-f).

The implicit and explicit schemes operate simultaneously in the model to represent both the subgrid scale and resolvable scale (mesoscale) precipitation processes. Zhang et al. (1989) show that this approach will handle mixed convective and stratiform precipitation systems and does not double count the effects of either resolvable scale or subgrid scale heating and moistening. Fig. 32 gives a trend line for the percentage ratio of non-convective to total rainfall along with the mean daily total rainfall as a function of

forecast lead time at 24-hours interval upto 3 days for each of the deep convection schemes. It can be seen that the total precipitation decreases with time for GD averaged across all the cases and for Gonu averaged across all the CPS schemes. However the fraction of grid-scale rainfall is shooting up significantly from day-1 to day-3 for KF and SAS schemes or for Sidr and Nargis cases whereas there is a decreasing trend of gridscale fraction for Gonu with forecast lead time. In general BMJ produced the least partitioning into convective and non-convective precipitation, which produces more or less uniform patterns over the region of rainfall with the least mesoscale variability.

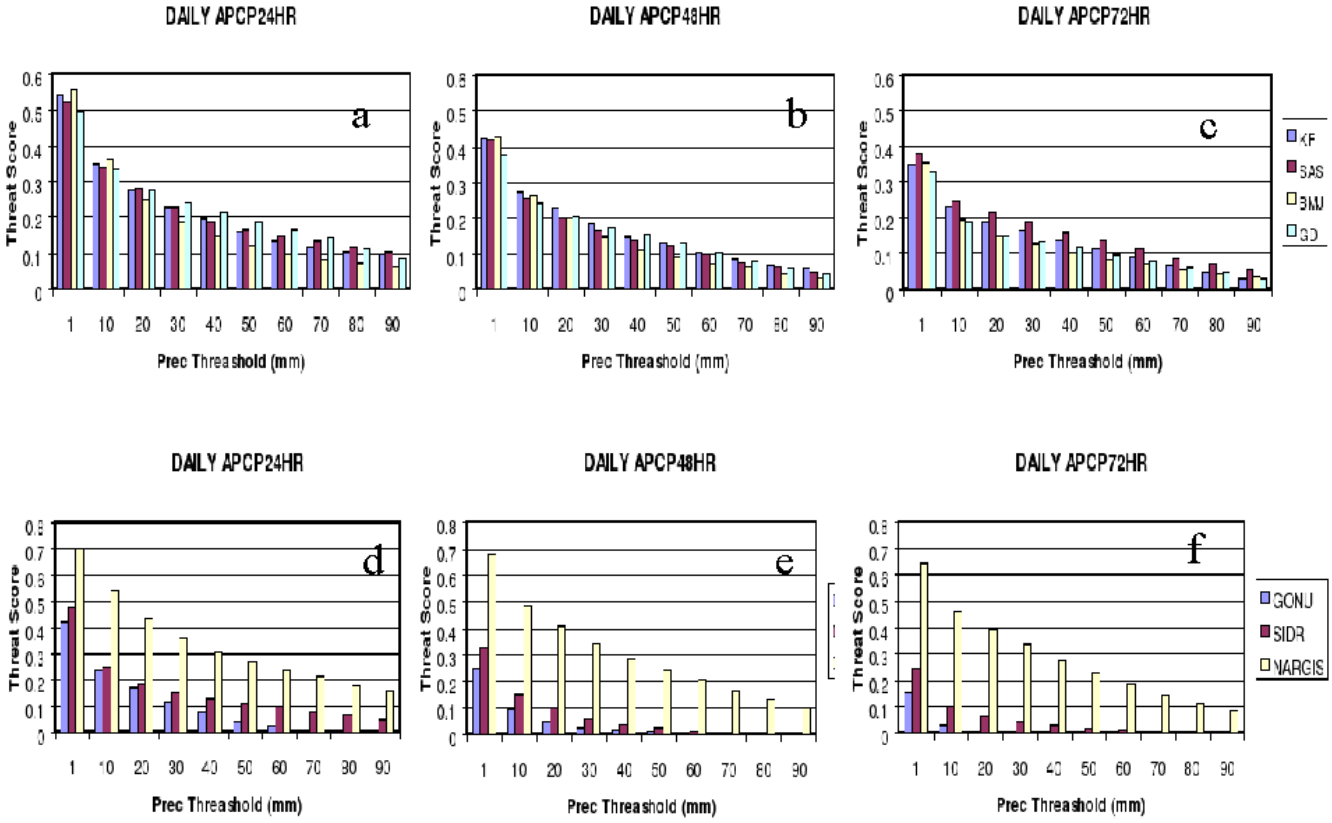

Fig. 28 Similar to Fig. 27, but for TS.

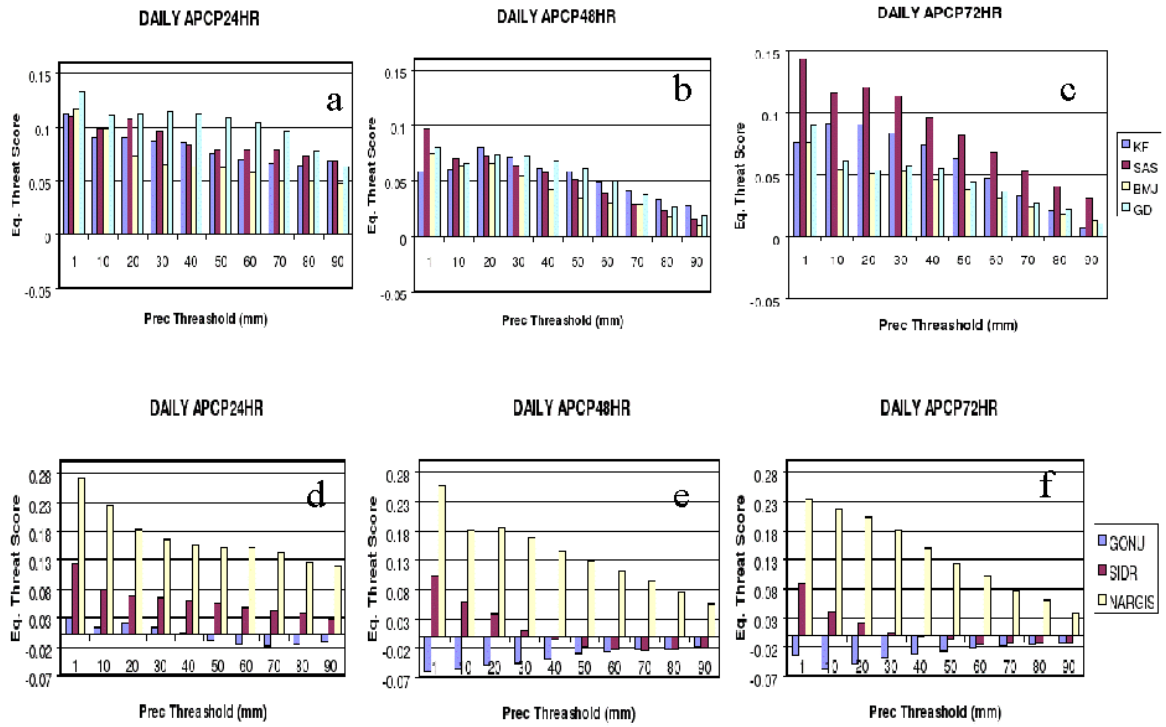

Fig. 29 Similar to Fig. 27, but for ETS.

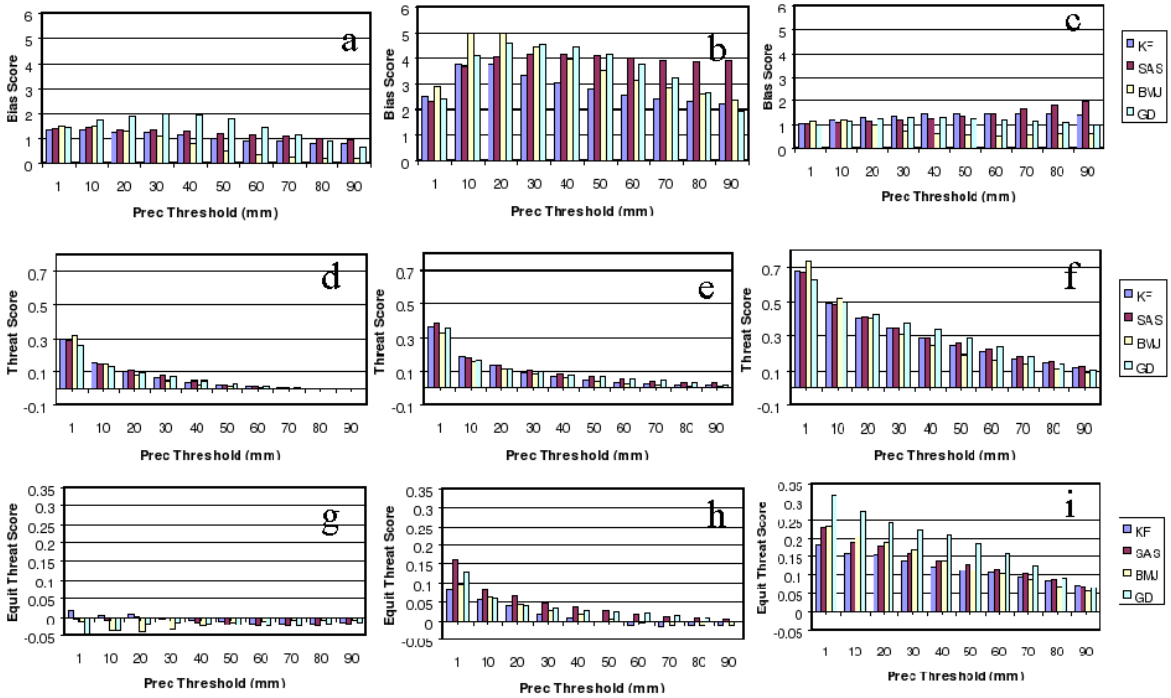

Fig. 30 BS, TS and ETS of total rainfall (mm/day) for various thresholds and for four CPS schemes for Gonu (a, d and g), Sidr (b, e and h) and Nargis (c, f and i).

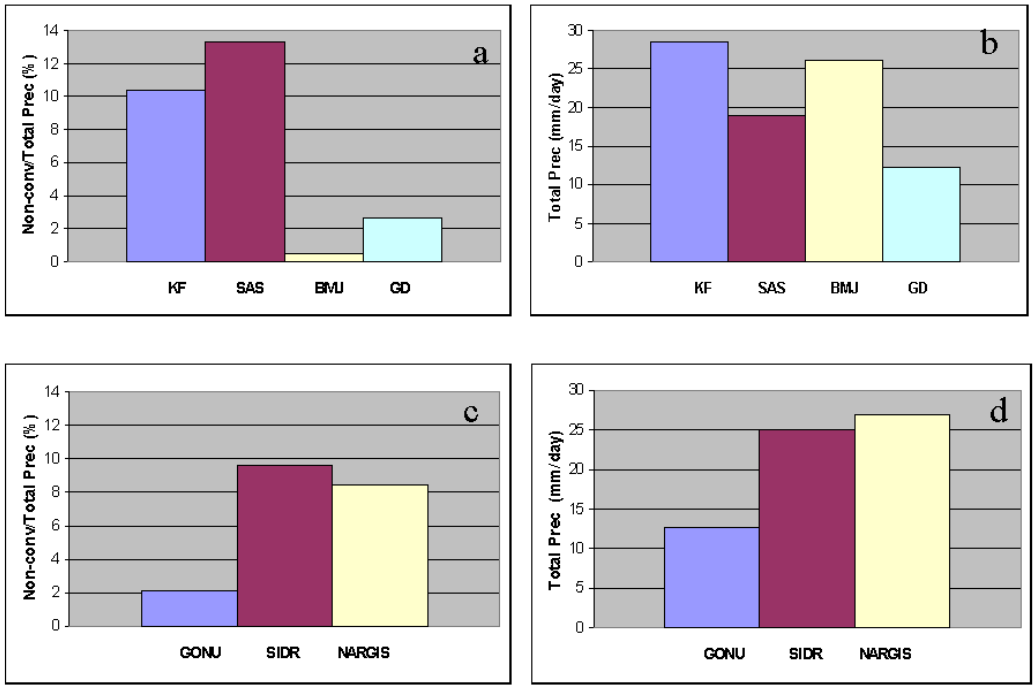

Fig. 31 Percentage ratio of Non-convective to total precipitation (a and c) along with mean total precipitation (b and d) in mm/day for 4 CPS schemes averaged across all cases (a and b) and across all CPS schemes (c and d).

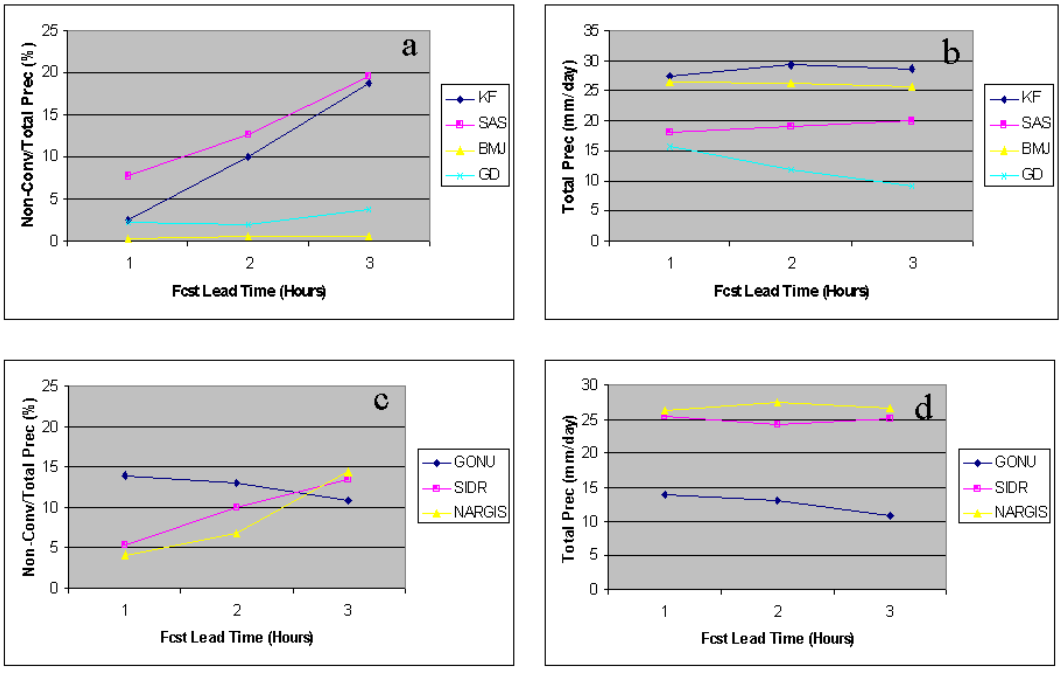

Fig. 32 Similar to Fig. 31, but curves connecting values of day-1 to day-3.

5. Summary

The current study compares the characteristic responses and errors associated with the CPS schemes and with respect to some particular synoptic conditions. Also the verification is not done for the entire integration domain, but only for a square grid box of each side 10 degrees in length around the centre of it, assuming that this area covers most of the associated features with respect to the particular TC under study. This may be another reason contributing to the relatively higher order of errors in statistical parameters compared to other studies as this region of associated rainfall may not entirely coincide with the region of actual rainfall as estimated by the TRMM estimates. So the emphasis has been given to the relative comparison between CPS schemes or cases rather than the absolute value of the parameters.

Part of the forecast errors depends on the physics, initial and boundary conditions and the synoptic conditions, like the region of formation, data availability to represent the actual pattern and intensity of the TC, accuracy and mesoscale details in initial conditions and the accuracy of the lateral boundary conditions (as in this case, the performance of the global model forecasts to which the WRF NMM is nested). These external parameters are identical for all CPS schemes for each case but relevant in case wise comparison. Track and intensity of the three cases chosen vary with the physics, integrations as well as the geographically related factors. The three cases are the unique examples in each of the factors and the forecast performances and hence the impact varies in each case. Sidr shows the maximum track error followed by Gonu in day-2 and day-3 and Nargis shows the least. Also comparison of track errors shows that KF produces the least errors averaged across all cases, though not much difference is seen on averaging for all the forecast lead times between KF, SAS and GD. BMJ performed poorest among the four when averaged across all the three cases.

Intensity and associated rainfall also vary from case to case with Nargis producing most intense patterns, KF trying to slightly over predict the intensity and GD

giving the least performance. Model failed to produce the observed intensity and the associated rainfall for Gonu cyclone. KF shows a tendency to over predict the peak gustiness in the spiral bands with the forecast lead time and produced the strongest convective organization, strongest narrow updraft and deepest moist troposphere in a column around the cyclonic centre, followed by SAS. GD in fact shows the weakest organization and spreading of energy over a large area and thus dissipates faster being unable to sustain the intensity. The standard rainfall verification scores also show a consistently better performance by the KF scheme. However it can be seen that the sensitivity of real-time model forecasts is equal or more to the external factors and synoptic conditions than the sensitivity between the CPS schemes itself. This is also applicable to the partitioning efficiency of the total precipitation into convective as well as grid-scale fractions. In general KF and SAS were found to be more efficient than BMJ and GD while the model showed least efficiency for Gonu, compared to Sidr and Nargis. Thus while evaluating the performance of the mesoscale models, one should keep in mind the synoptic environments and the initial and boundary conditions.

In general, most of the CPS scheme performances will not vary much under strong synoptic forcings. But there can be a wide range of performance variations and feedbacks under weak synoptic forcings. At a resolution of about 27Km, KF is found to be the best among the CPS schemes as far as TCs over Indian ocean basin are concerned, in simulating the near-realistic observed intensity. This conclusion can not be generalized in all the TC cases or all other basins, but many examples of recent studies have brought up similar conclusions. Also it can not be stated that any single CPS scheme can be identified to perform better in all types of rainfall events or synoptic conditions. Many studies have shown sensitivity of cumulus convection to the location and intensity of the circulation and precipitation and to the partition of grid-scale and subgrid-scale precipitation. An important feature which can be noticed is that KF and SAS produces more fraction of grid-resolvable component of precipitation, whereas BMJ and GD produces very negligible fraction. Also the grid scale component of rainfall shows an increasing trend alongwith the model integration for KF and SAS and also for Sidr and Nargis cases, whereas GD or for Gonu system shows a decreasing trend. The current study finds that during the stronger synoptic forcings, the grid-scale component to rainfall production increases and the feedback processes result into a better organization and buildup.

Acknowledgements

Global and mesoscale models mentioned in this study are adopted versions from National Centre for Environment Prediction (NCEP), USA. Rainfall observations are derived daily TRMM precipitations and observed tracks of the three tropical cyclone cases are obtained from India Meteorological Department (IMD).

References

Betts, A. K., and M. J. Miller, 1993: The Betts–Miller scheme. The Representation of Cumulus Convection in Numerical Models, Meteor. Monogr., No. 46, Amer. Meteor. Soc., 159–164.

Cram, J. M., R. A. Pielke, and W. R. Cotton, 1992: Numerical simulation and analysis of a prefrontal squall line. Part I: Observations and basic simulation results. J. Atmos. Sci., 49, 189–208.

Dudhia, J., 1989: Numerical study of convection observed during the winter monsoon experiment using a mesoscale two-dimensional model, J. Atmos. Sci., 46,3077-3107.

Deb, SK, TP Srivastava, and CM Kishtawal, 2008: The WRF performance for the simulation of heavy precipitating event over Ahmedabad during August 2006. J. Earth Sys. Sci., 117, 589-602.

Frank, WM, 1983: The cumulus parameterization problem. Mon. Wea. Rev., 111, 1859-1871.

Gallus, W.A., Jr., 1999: Eta simulations of three extreme precipitation events: Sensitivity to resolution and convective parameterization, Wea. Forecasting, 14, 405-426.

Grell, G.A., 1993: Prognostic evaluation of assumptions used by cumulus parameterizations, Mon. Wea. Rev., 121, 764-787.

Grell, G.A, J. Dudhia, and D.R. Stauffer, 1994: A description of the fifth generation Pen State/NCAR Mesoscale Model (MM5), NCAR Tech. Note NCAR/TN-398+STR, 138 pp.

Grell, GA, and D Devenyi, 2002: A generalized approach to parameterizing convection combining ensemble and data assimilation techniques, Geoph. Res. Let., 29, NO 14.

Houze, R.A., Jr., 1977: Structure and dynamics of a tropical squall line system, Mon. Wea. Rev., 105, 1541-1567.

Janjic, ZI, 1994: The step-mountain eta coordinate model: further developments of the convection, viscous sublayer and turbulence closure schemes. Mon. Wea. Rev., 122, 927-945.

Janjic, ZI, 2000: Comments on "Development and Evaluation of a Convective Scheme for Use in Climate Models", J. Atmos. Sci., 57, p. 3636.

Johnson, R.H., and P.J. Hamilton, 1988: The relationship of surface pressure features to the precipitation and air flow structure of an intense midlatitude squall line, Mon. Wea. Rev., 116, 1444-1472.

Kain, JS, 2004: The Kain-Fritsch Convective Parameterization. An Update. J. Appl. Meteor., 43, 170-181.

Kain, JS, and JM Fritsch, 1990: A one-dimensional entraining/ detraining plume model and its application in convective parameterization. J. Atmos. Sci., 47, 2784-2802.

Kain, JS, and JM Fritsch, 1993: Convective parameterization for mesoscale models: The Kain-Fritsch scheme. The representation of cumulus convection in numerical models, K. A. Emanuel and D.J. Raymond, Eds., Amer. Meteor. Soc., 246 pp.

Kuo, Y.-H., R.J. Reed, and Y. Liu, 1996: The ERICA IOP 5 Storm. Part III: Mesoscale cyclogenesis and precipitation parameterization, Mon. Wea. Rev., 124, 1409-1434.

Ma, L.-M, and Z.-M. Tan, 2009: Improving the behavior of the cumulus parameterization for tropical cyclone prediction: Convection trigger, Atmos. Res., 92, 190-211.

Marchok, T, R Rogers and R Tuleya, 2007: Validation schemes for tropical cyclones quantitative precipitation forecasts: Evaluation of operational models for U.S. landfalling cases. Wea. Forecasting, 22, 726-746.

Molinari, J., and M. Dudek, 1992: Parameterisation of convective precipitation in mesoscale numerical models: A critical review, Mon. Wea. Rev., 120, 326-344.

Pan, H-L, and W-S Wu. 1995: Implementing a Mass Flux Convection Parameterization Package for the NMC Medium-Range Forecast Model. NMC Office Note, No. 409, 40pp. [Available from NCEP, 5200 Auth Road, Washington, D.C. 20233].

Peng, X., and K. Tsuboki, 1997: Impact of convective parameterizations on mesoscale precipitation associated with the Baiu front, J. Meteor. Soc. Japan, 75, 1141-1154.

Rajagopal, E.N., M. Dasgupta, S. Mohandas, J.P.George, G.R. Iyengar, and D.P. Kumar, 2007: Implementation of T254L64 Global Forecast System at NCMRWF, NCMRWF Technical Report NMRF/TR/1/2007, NCMRWF (Min. Earth Sciences), A-50, Sector-63, Noida, May 2007, 42 pp.

Rao, DVB and DH Prasad, 2007: Sensitivity of tropical cyclone intensification to boundary layer and convective processes, Natural Hazards, 41, 429– 445.

Simpson, J.S., C. Kummerow, W.-K. Tao, and R.F. Adler,1996: On the Tropical Rainfall Measuring Mission (TRMM), Meteorol. Atmos. Phys., 60, 19-36.

Spencer, P.L., and D.J. Stensrud, 1998: Simulating flash flood events: Importance of the subgrid representation of convection, Mon. Wea. Rev., 126, 2884-2912.

Stensrud, D. J., J.-W. Bao, and T.T. Warner, 2000: Using initial conditions and model physics perturbations in short-range ensemble simulations of mesoscale convective systems, Mon. Wea. Rev., 128, 2077-2107.

Stensrud, D. J., and J. M. Fritsch, 1994: Mesoscale convective systems in weakly forced large-scale environments. Part III: Numerical simulations and implications for operational forecasting. Mon. Wea. Rev., 122, 2084–2104.

Vaidya, SS, 2007: Simulation of weather systems over Indian region using mesoscale models, Meterol. Atmos. Phys., 95, 15 – 26.

Vaidya, SS and JR Kulkarni, 2007: Simulation of heavy precipitation over Santacruz, Mumbai on 26 July 2005, using mesoscale model, Meterol. Atmos. Phys., 98, 55 – 66.

Wei Wang and NL Seaman, 1997: A comparison study of convective parameterization schemes in a mesoscale model, Mon. Wae. Rev., 125, 252 – 278.

Yang, M.-J., and Q.-C. Tung, 2003: Evaluation of rainfall forecasts over Taiwan by four cumulus parameterization schemes, J. Meteorol. Soc. Japan, 81, 1163-1183.

Yang, M.-J., F.-C. Chien, and M.-D. Cheng, 2000: Precipitation parameterizations in a simulated Mei-Yu front, Terr., Atmos. And Oceanic Sci., 11, 393-422.

Zhang, D.-L., 1989: The effect of parameterized ice microphysics on the simulation of vortex circulation with a mesoscale hydrostatic model, Tellus, 41A, 132-147.

Zhang, D.-L, K. Gao, and D.B. Parsons, 1989: Numerical simulation of an intense squall line during 10-11 June 1985 PRE-STORM.Part I: Model verification, Mon. Wea. Rev., 117, 960-994.

Zheng, Y., Q. Xu, and D. J. Stensrud, 1995: A numerical simulation of the 7 May 1985 mesoscale convective system. Mon. Wea. Rev., 123, 1781–1799.

----------0---------